[32]C. A. Fenstermacher, J. E. Draper, and C. K. Bockelman, Nucl. Phys. 10, 386 (1959).
[33]J. R. Huizenga and R. Vanderbosch, Phys. Rev. 120, 1035 (1960).
[34]W. P. Pönitz, Z. Physik, 197, 262 (1966).
[35]D. Sperber and J. W. Mandler, Nucl. Phys. A113, 689 (1968).
[36]K. J. Wetzel and G. E. Thomas, Phys. Rev. C 1, 1501 (1970).
[37]M. R. Bhat, R. E. Chrien, D. I. Garber, and O. A. Wasson, Phys. Rev. (to be published).
[38]M. D. Goldberg, S. F. Mughabghab, S. N. Purohit, B. A. Magurno, and V. M. May, Brookhaven National Laboratory Report No. BNL 325, 1966 (unpublished), 2nd ed., Suppl. 2.

PHYSICAL REVIEW C VOLUME 2, NUMBER 2 AUGUST 1970

Intermediate Structure in the Photon Interaction Cross Sections of Sn and Zr†

P. Axel, K. K. Min,* and D. C. Sutton
Physics Department, University of Illinois, Urbana, Illinois 61801
(Received 2 February 1970)

Photon scattering cross sections were measured with 70-keV resolution from 6 to 9 MeV in Sn, and from 8.5 to 12.5 MeV in Zr. A new method of analysis is used to infer relatively reliable total photon interaction cross sections. Both the elastic scattering and the total interaction cross sections vary more rapidly with energy than had been anticipated; the best identified localization of transition strength is between 11.4 and 11.8 MeV in Zr. The average total interaction cross sections are qualitatively similar to, but about 50% larger than, an extrapolation of the electric dipole giant resonance. The cross sections are large enough to imply that electric dipole interaction dominates at most energies. The relative probability of photon scattering and photoproton emission is very sensitive to correlations between proton widths and ground-state γ-ray widths. There is no evidence for width correlations associated with the additional strength concentrated near 11.5 MeV in ^{90}Zr.

I. INTRODUCTION

The elastic scattering of photons at energies near and below the neutron emission threshold can provide valuable new insights into several different aspects of nuclear structure. This paper will show that the observed elastic scattering can be used to obtain a reliable estimate of the total photon interaction cross section. Elastic-scattering experiments therefore make it possible to extend our knowledge of photon interactions to lower energies than can be reached with other techniques. This extension is important in order to bridge the gap between the region of the electric dipole giant resonance and very low energies which dominate nuclear γ-ray cascades.

Photon interactions in this energy region are also especially interesting because they reveal the way in which a simple nuclear excitation is shared by many neighboring complicated nuclear states. At most energies the photon cross sections measure that component of the excited states which can be reached by electric dipole absorption. Inasmuch as this component can be determined over a relatively large energy range, photon interactions should be helpful in learning more about intermediate structure.

Energy regions which consist of nonoverlapping levels have special advantages in the study of intermediate structure. Each level contributes to average cross sections in accordance with its partial widths. If one type of partial width is larger in some energy region, the levels in that region must have a larger amount of the corresponding nuclear configuration. If some nuclear configuration contributes importantly to two partial widths, these widths will be correlated. This paper will show that when photoproton emission provides the main competition for photon scattering, this scattering is exceptionally sensitive to width correlations.

Correlations between partial widths of nonoverlapping levels merit much more study than they have received. The nonoverlapping levels are well understood quasistationary quantum states whose modes of decay are independent of the modes of formation. However, the width correlations have the interesting effect of favoring some average partial cross sections disproportionately when compared with the corresponding average widths. In this sense, the correlations can be thought of as the low-energy forerunners of quasidirect, nonstatistical processes which are usually discussed as being the early temporal stages of a nuclear interaction.

There is little experimental or theoretical infor-

mation about the energy dependence of photon interactions near and below the neutron threshold. Elastic photon scattering was measured below neutron thresholds in a few cases,[1-4] but only with either poor energy resolution[1,3,4] or nonvariable energy.[2] These early measurements were not inconsistent with the qualitative expectation[5] of a photon interaction which rises smoothly as the energy approaches the giant dipole resonance. (The photon scattering cross section drops abruptly just above the neutron threshold because photoneutron emission becomes dominant.) However, the elastic-scattering cross sections had not been analyzed quantitatively, nor had reliable total cross sections been inferred.

One important ingredient in the understanding of photon interactions below the neutron threshold is an adequate analysis of the effects on average cross sections of the variations in partial widths from level to level. Effects of width variations on some other nuclear reactions had been considered,[6,7] and the semiquantitative implications of these variations on photon interactions were discussed earlier.[8] A more quantitative discussion is given in this paper; it will be shown that these width variations can have much larger effects on some average cross sections than had been appreciated.

When the effects of width variations were taken into account semiquantitatively, it became clear[8] that elastic photon scattering and resonant absorption results were consistent both with photoneutron cross sections and with the studies of the high-energy γ rays which are emitted after the capture of slow neutrons. The magnitude of the photon interaction cross section near 7 MeV was shown[8] to be in approximate agreement with an extrapolation to low energy of a classical Lorentz line adjusted to fit the giant resonance cross section.

More recent data confirm this conclusion. The low-energy photoneutron cross sections are reasonably well described by a Lorentz line adjusted to fit the giant resonance region. Since 1962, the absolute photoneutron cross sections have been revised downward from what had been accepted in 1962, and hence the numerical estimates given then[8] should be decreased by a factor which may be as large as 1.4. (Sum-rule predictions including exchange effects are about 1.4 times the classical sum rule; in 1962, it was believed that the entire sum-rule prediction, including exchange was observed in the giant resonance. It now appears, experimentally, that the integrated cross section in the giant resonance region of medium and heavy nuclei is sometimes as low as the classical sum rule without exchange.) This numerical change brings the extrapolated values into even better agreement with capture γ-ray data which were reviewed recently by Bollinger.[9]

Despite the apparent success of the empirical extrapolation of photon interaction cross sections from the giant resonance to lower energies, there has been no theoretical guidance for this extrapolation. The width of the giant resonance is not understood, and the validity of parametrizing the observed cross section as though it were a classical damped oscillator has never been established. It is therefore not surprising that the interpretation of low-energy photon interactions has remained uncertain; so small a cross section will not be predictable until the theories which purport to explain the dominant features of the electric dipole giant resonance are refined considerably. Measurements of low-energy photon interaction cross sections should provide some hints to guide the required theoretical improvements.

The experiments described below were initiated with the intention of using the 70-keV resolution of the Illinois-bremsstrahlung monochromator[10,11] to measure the energy dependence of the photon scattering cross section. We had also intended to do some auxiliary experiments to learn about other partial cross sections and the level parameters. Zr was selected for investigation because its most abundant isotope, ^{90}Zr, has a very high-neutron threshold (i.e., above 11.9 MeV), and a relatively large level spacing which enhances elastic scattering.[12] Assuming that the other Zr isotopes do not contribute significantly to the elastic scattering at energies above their neutron thresholds, our measurements give information about ^{90}Zr over a 4-MeV energy region, one end of which is only about 4 MeV from the peak of the ^{90}Zr giant resonance.[13]

The experimental emphasis was changed when we observed unanticipated rapid variations of the elastic-scattering cross section with energy. When it became clear that the cross section was not a slowly varying function of energy, it became impractical to do the auxiliary experiments needed to obtain either other partial cross sections or a precise value for the total cross section. Instead, we concentrated on showing that the rapid variations actually existed. In addition, we decided to study a natural mixture of the many Sn isotopes to see whether any rapid variations would be observable despite the addition of contributions from several different isotopes.

The existence of the unexpected rapid energy dependence of the photon scattering was reported in a Letter,[14] which pointed out that these effects were observed in ^{206}Pb and ^{209}Bi, as well as in ^{90}Zr and Sn. Although an "intermediate resonance model" had been suggested[15] to explain rapidly varying cross sections in other types of reactions at higher energy, this model did not appear to be applicable

to the clustering of transition strength which we observed. At about the same time that our Letter was published,[14] a number of theoretical papers[16] introduced the concepts of "doorway states" and "intermediate structure." The experimental reports of rapid energy dependences of various reaction cross sections which followed are too numerous to mention; some of them are discussed in a review[17] of intermediate structure. Despite the popularity of this aspect of nuclear physics, very little is known about the spreading of a simple excitation among the complicated nuclear levels.[18] The energy variation of the photon interaction cross section continues to be among the most promising examples of concentrations of transition strength. The theoretical framework of intermediate structure[17] can probably accommodate whatever mechanism is responsible for cross-section maxima such as we observe; however, up to this time, intermediate structure has provided only a name, rather than a semiquantitative explanation for the strength concentrations implied by our data.

After our experiment had been completed, some related results became available[19-21] from studies of the ground-state γ rays emitted after proton capture by ^{89}Y. These data, with the aid of detailed balance, provided a direct measure of the photoproton cross section. The combination of the photoproton and the elastic photon scattering cross sections are used in this paper to obtain a reliable estimate of the total photon interaction cross section, and to confirm its rapid energy variation. In addition, the competition between elastic photon scattering and photoproton emission can provide an exceptionally sensitive test for possible correlations of partial widths for γ-ray and proton emission.

This sensitivity arises, in part, because the average proton width exceeds the average γ-ray width, and, in part, because the incident γ rays selectively populate levels with larger than average ground-state γ-ray widths. If these γ-ray widths and the proton widths are distributed according to two independent Porter-Thomas distributions, there is a significant probability that levels, including those with large γ-ray widths, have proton widths that are considerably below average. Thus, in the absence of correlations, the ratio of elastic scattering to photoproton emission is considerably greater than the ratio of the average widths, $\langle\Gamma_{\gamma 0}\rangle/\langle\Gamma_p\rangle$. This effect is described in more detail in the Appendix, where it is shown that the enhancement factor in the cross-section ratios can be as large as $1+2(\langle\Gamma_p\rangle/\langle\Gamma_{\gamma 0}\rangle)^{1/2}$. On the other hand, if the partial widths were completely correlated in some energy region, the elastic-scattering cross section would drop to its unenhanced value so that $\sigma_{\gamma\gamma}/\sigma_{\gamma p} = \langle\Gamma_{\gamma 0}\rangle/\langle\Gamma_p\rangle$. Some numerical examples will be given in Sec. IV C 3 when the ^{90}Zr data are discussed.

The sensitivity of $\sigma_{\gamma\gamma}/\sigma_{\gamma p}$ to correlations between partial proton and ground-state γ-ray widths provides a welcome additional method of studying such correlations. Recent neutron capture γ-ray studies[9,22] suggest a correlation between the reduced neutron widths and the probabilities of emitting high-energy γ rays in the ^{169}Tm(n,γ) reaction; this correlation has been studied over a very small energy range. For nuclei in which proton emission dominates, the comparison of $\sigma_{\gamma\gamma}$ and $\sigma_{\gamma p}$ can be particularly informative because this comparison can be extended over a wider energy region than is accessible for neutron capture γ-ray studies. It will be shown that the combination of $\sigma_{\gamma\gamma}$ and $\sigma_{\gamma p}$ implies a reliable value for the ground-state γ-ray strength function, $\Gamma_{\gamma 0}/D$. If the proton strength function, Γ_p/D, were known accurately from other measurements (e.g., from reliable optical-model parameters), the degree of correlation between $\Gamma_{\gamma 0}$ and Γ_p could be inferred. If Γ_p/D is not known with sufficient reliability, the combination of $\sigma_{\gamma\gamma}$ and $\sigma_{\gamma p}$ sets limits on Γ_p/D; the precise value of Γ_p/D depends on the amount of correlation.

Our photon scattering experiment is described in Sec. II, and our results are given in Sec. III. The quantitative relations between the observed scattering and the level parameters are given in Sec. IV A and in the Appendix. These relations are used in interpreting our results in Sec. IV B. The conclusions are summarized in Sec. IV C.

II. EXPERIMENTAL TECHNIQUE

A. Monochromatic γ-Ray Beam

The bremsstrahlung monochromator has been described,[10,11] and most of the experimental details were essentially those used in a previous experiment.[11] An electron beam of energy, E_β, is extracted from the University of Illinois 25-MeV betatron and is energy analyzed by a deflecting magnet. It then strikes a bremsstrahlung converter which is in the source position of a β-ray spectrometer[23]; this spectrometer measures the energy, E_e, of the postbremsstrahlung electron. The detection of a postbremsstrahlung electron by any one of three separate scintillators ($3.8\times1.5\times0.8$ cm, Pilot B) announces the production of a "tagged" γ ray of energy $E_\gamma = E_\beta - E_e$. A coincidence circuit was used to select only those scattered γ rays which gave a signal within about a 12-nsec time interval defined by the detected electron.

The detected scattered γ rays which were in coincidence with an electron were not necessarily produced by the corresponding monochromatic γ ray because at the counting rates used there was a

significant probability that an electron detector would be detecting an electron at the same time that, by chance, an unrelated γ ray was detected. For example, with a typical electron detector counting rate of 2×10^4 electrons/sec, the average time between electrons is about 1.8 μsec during the 200-μsec long-beam pulses which recur 180 times per sec. If each detected electron corresponds to a 12-nsec sensitive time, the probability that a random γ ray would produce a coincidence output is (12 nsec/1.8 μsec) $= 6.7\times10^{-3}$. This random probability is measured with high precision to provide an accurate correction for chance coincidences despite fluctuations in the electron intensity. This random probability was usually about 10^{-2}; for the measurements being reported, this corresponds to about an equal number of chance events and true events at the average values of the cross sections.

The chance coincidence background limited the acceptable beam intensity to about 2×10^4 electrons per sec which corresponds to about 10^4 monochromatic γ rays striking the scatterer per sec. These γ rays are confined to an energy interval of about 70 keV. The exact resolution of the monochromator was not studied because it is unimportant for the results to be reported. An estimate of the resolution will be given for each experimental point. Three γ-ray energies were studied simultaneously with the aid of the three independent electron detectors. The absolute energy scale was determined by a calibration procedure which should have identified the energy to about 30 keV. However, in view of the higher accuracy of the photoproton cross-section energy scale, an improved calibration will be made. The actual average total electron current incident on the converter was about 10^{-9} A. Most of these electrons pass through the thin converter with essentially no energy loss; they are deflected by the spectrometer and stopped in a paraffin beam stop. The total background contributed by these electrons and by γ rays which did not strike the scatterer was only about 15% of the total detected number of scattered γ rays when a scatterer was in place.

B. Cross-Section Determination

The scattered γ rays whose energy was within about 15% of the incident energy beam were detected by a 5-in. diam $\times$ 4-in. thick NaI crystal at 135°. Because of the relatively poor energy resolution of the NaI, the observed scattering may have included some inelastic scattering, and is therefore called quasi-elastic. The scatterers contained 4.6×10^{22} atoms/cm^2 of Zr (in the form of ZrO_2) and 5.5×10^{22} atoms/cm^2 of Sn. The normal to the ZrO_2 target made an angle of 22.5° with respect to the incident γ-ray beam while the normal to the Sn sample made an angle of 45° (i.e., the Sn sample was parallel to the NaI detector).

The absolute values of the differential quasi-elastic scattering were limited by statistical accuracy and not by other experimental uncertainties. As in previously reported scattering experiments,[10,11] we reduced the possible errors in detector efficiency by using the same detector to measure the incident beam and the scattered γ rays. The wider angular divergence of the scattered γ-ray beam introduced a correction which was equivalent to reducing the effective solid angle by multiplying the actual geometric solid angle subtended by the detector, Ω_{dg}, by a factor, c, which was 0.75, 0.76, and 0.71 at 7.5, 9.5, and 11.5 MeV, respectively. The effective solid angle (i.e., $c\Omega_{dg}$) was 0.172 sr at 7.5 MeV.

As developed in more detail in earlier publications[10,11] the quasi-elastic differential cross section can be expressed as

$$\frac{d\sigma}{d\Omega} = \frac{1}{\mathfrak{N}_{\mathrm{eff}}}\frac{N_t}{N_{\gamma\mathrm{eff}}}\frac{1}{c\Omega_{dg}},$$

where c and Ω_{dg} were discussed above, N_t is the number of true coincidences, $\mathfrak{N}_{\mathrm{eff}}$ is the effective number of target nuclei, and $N_{\gamma\mathrm{eff}}$ is the "effective" number of incident γ rays. Atomic processes leading to quasi-elastic scattering are unimportant at backward angles. The observed average cross sections were of the order of 0.3 mb/sr, and hence much greater than the 0.01 mb/sr expected for Thomson scattering by the total nuclear charge.

The number of true coincidences, N_t, was obtained by subtracting the chance coincidences from the observed coincidences; the determination of chance coincidences was described in Sec. II D of Ref. 11. The effective number of γ rays, $N_{\gamma\mathrm{eff}}$, is defined as the product of the number of "tagged" γ rays which are produced, the probability that the γ ray will strike the sample, and the γ-ray detection efficiency. This combination of parameters is combined in one symbol because the number of effective γ rays per detected electron can be measured directly by placing the detector in the sample position in the incident γ-ray beam (as described in more detail in Sec. II E of Ref. 11).

$\mathfrak{N}_{\mathrm{eff}}$ is the effective number of atoms/cm^2 (perpendicular to the beam) which contributed to the observed scattering. This effective number was defined to be less than the actual number by the energy dependent factor which allows for atomic absorption effects. In arriving at the number of effective atoms, assumptions were made about which isotopes contributed to the nuclear scattering. For ZrO_2, it was assumed that only Zr^{90} and Zr^{92} contributed to the scattering below 8.7 MeV, and that only Zr^{90} contributes above 8.7 MeV (which is the

neutron emission threshold for Zr^{92}). For Sn, it was assumed that at each energy only those isotopes contributed whose neutron thresholds were at higher energies. The fraction of Sn atoms assumed to contribute are given in Table I. For example, from 7.54 to 8.51 MeV, the observed average cross sections were divided by 0.835; note that up to 9.11 MeV this factor remained at or above 0.728. No correction was made for nuclear absorption of the γ rays in the scatterer. Experimental absorption data at 7.2 MeV indicated that an Sn absorber twice the thickness of the Sn scatterer would cause about a 25% nuclear absorption so that the mean absorption in the scatterer might have been about 6% at that energy. This absorption would imply that the true scattering cross section for Sn at 7.2 MeV is about 6% higher than the value given below. Since it is reasonable to expect the nuclear absorption to be less important as the energy increases, the error involved in neglecting nuclear absorption is small. The nuclear absorption was also neglected for Zr, in which case a 15-h self-absorption measurement at 11.5 MeV (where the scattering was particularly large) gave no detectable absorption. (This measurement does not exclude the possibility of absorption effects at lower energy, but the level parameters inferred in Sec. IV B suggest that the absorption would not be expected to be more than 2 times as large at 9 MeV.)

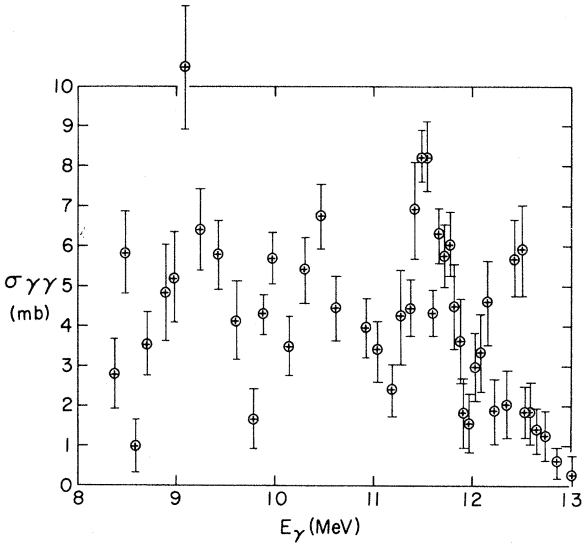

FIG. 1. The photon elastic-scattering cross section of Zr. The values assume that only ^{90}Zr contributes above 8.68 MeV. Numerical values are given in Table II.

III. EXPERIMENTAL RESULTS

The experimental quasielastic scattering cross sections, $\sigma_{\gamma\gamma}$, obtained for Zr and Sn are listed in Tables II and III and shown in Figs. 1 and 2. (The angular distribution was assumed to be $1+\cos^2\theta$ as expected for a $0\rightarrow 1\rightarrow 0$ transition.) The resolutions (ΔE_γ) given in the tables are estimates of the full width at half maximum of a complicated and inexactly known resolution function. (The anomalously large values of the resolution arise from averaging two neighboring runs to improve statistics.) For Zr, the cross section was computed assuming that 68.6% of the Zr contributed to the scattering below 8.68 MeV (i.e., Zr^{90} and Zr^{92}) while 51.5% contributed above 8.68 MeV. The fraction of Sn isotopes assumed to contribute to the cross section is listed in Table III. Also listed in Table III, as the uncorrected cross section, is the value which would be appropriate if 100% of the Sn isotopes were to contribute to the observed scattering at all energies. These uncorrected values are also shown (as dots) in Fig. 2 together with the corrected values. A comparison of the uncorrected and corrected cross sections in Fig. 2 makes it clear that the rapid variations of cross sections with energy are not significantly affected by the assumptions about which isotopes contribute.

Previously reported experimental results in the same energy region are available for Sn, but not for Zr. The good resolution measurements of

TABLE I. Abundances and photoneutron thresholds of tin isotopes.

A	% abundance	(γ,n) threshold (MeV)	Fraction of Sn with (γ,n) threshold equal to or greater than energy in column three
119	8.58	6.48	1.0
117	7.57	6.94	0.914
115	0.34	7.54	0.838
124	5.98	8.51	0.835
122	4.71	8.80	0.775
120	32.97	9.11	0.728
118	24.01	9.33	0.398
116	14.24	9.56	0.158
114	0.65	10.32	0.016
112	0.95	11.08	0.009

TABLE II. Photon cross sections for ^{90}Zr. See Sec. III for an explanation of the headings and entries in this table.

E_γ (MeV)	ΔE_γ (keV)	$\sigma_{\gamma\gamma}$[a] (mb)	$\sigma_{\gamma p_0}$[b] (mb)	$\sigma_{\gamma t}$[a] (mb)	Single-particle units per MeV
8.38	60	2.79 ± 0.90		5.2 ± 1.4	0.047
8.49	60	5.84 ± 1.03		9.2 ± 1.5	0.082
8.60	60	1.00 ± 0.69		2.8 ± 1.5	0.024
8.70	110	3.55 ± 0.80		6.5 ± 1.2	0.055
8.89	60	4.84 ± 1.22		8.5 ± 1.6	0.068
8.98	60	5.21 ± 1.15		9.1 ± 1.5	0.072
9.09	60	10.51 ± 1.61		15.8 ± 2.3	0.125
9.24	60	6.38 ± 0.95		11.1 ± 1.3	0.083
9.43	120	5.78 ± 0.87		10.6 ± 1.2	0.076
9.61	60	4.14 ± 0.99		8.7 ± 1.5	0.061
9.79	60	1.68 ± 0.76		5.0 ± 1.5	0.033
9.88	70	4.31 ± 0.49		9.5 ± 0.8	0.063
9.98	70	5.70 ± 0.63		11.7 ± 1.0	0.075
10.14	110	3.48 ± 0.74		8.9 ± 1.3	0.055
10.31	70	5.40 ± 0.85		12.1 ± 1.3	0.073
10.46	80	6.75 ± 0.08		14.6 ± 1.2	0.085
10.62	120	4.45 ± 0.78	1.1	11.9 ± 1.3	0.056
10.92	70	3.95 ± 0.73	3.1	13.0 ± 1.3	0.069
11.04	70	3.39 ± 0.76	3.7	12.7 ± 1.4	0.067
11.20	70	2.41 ± 0.66	3.8	11.1 ± 1.6	0.057
11.28	70	4.28 ± 1.15	5.3	16.3 ± 2.2	0.082
11.38	70	4.48 ± 0.73	6.8	17.9 ± 1.3	0.088
11.42	70	6.88 ± 1.19	6.3	20.6 ± 2.0	0.100
11.49	70	8.20 ± 0.66	8.0	25.7 ± 1.1	0.124
11.54	70	8.20 ± 0.88	7.5	25.4 ± 1.6	0.122
11.60	70	4.33 ± 0.57	8.6	19.6 ± 1.2	0.095
11.66	70	6.28 ± 0.67	8.1	22.9 ± 1.2	0.109
11.71	70	5.75 ± 0.80	7.7	21.8 ± 1.4	0.101
11.78	70	6.05 ± 0.80	10.7	25.0 ± 1.5	0.116
11.82	70	4.50 ± 1.04	9.6	21.3 ± 2.1	0.098
11.88	70	3.63 ± 1.08	9.5	19.5 ± 2.4	0.089
11.92	70	1.85 ± 0.87	9.9	16.2 ± 1.7	0.073
11.98	70	1.55 ± 0.74	12.4	17.7 ± 2.0	0.079
12.04	70	2.99 ± 0.87	12.3	21.2 ± 1.6	0.093
12.09	70	3.33 ± 0.97	10.2	19.9 ± 2.4	0.088
12.16	70	4.60 ± 1.08	11.6	24.3 ± 2.3	0.105
12.23	70	1.88 ± 0.81	13.0	19.4 ± 2.1	0.083
12.35	70	2.05 ± 0.84	12.3	19.5 ± 2.2	0.082
12.42	70	5.71 ± 0.94	14.0	29.4 ± 1.8	0.122
12.47	70	5.91 ± 1.14	14.4	30.0 ± 2.3	0.124
12.54	80	1.85 ± 0.64	12.0		
12.58	80	1.85 ± 0.81	10.2		
12.66	80	1.38 ± 0.57	8.6		
12.74	80	1.28 ± 0.64			
12.86	80	0.60 ± 0.40			
13.01	80	0.27 ± 0.50			

[a] Assuming that ^{90}Zr and ^{92}Zr have equal cross sections below 8.68 MeV and that only ^{90}Zr contributes above 8.68 MeV. The listed errors include only the effects of the statistical uncertainty in the number of scattered γ rays.

[b] The photoproton cross sections were calculated from the graphs of the p,γ_0 reaction in Refs. 19 and 20. An isotropic angular distribution was assumed. The cross section in Ref. 20 was used to obtain an absolute scale for the data of Ref. 19 near 12-MeV excitation. In accordance with a private communication from Rauch, it was assumed that the detector used in Ref. 19 decreased in efficiency with increasing energy by 5% per MeV. Above 11.95 MeV, the photoproton cross sections are averages of the precise, very good resolution data of Ref. 20 over 100-keV intervals; the relative cross sections in this energy region should have negligible error. The reliability of the relative cross sections at lower energy appears to be of the order of or less than 10%. For example, there are local maxima at about 11.36, 11.45, and 11.63 MeV which are about 10% and which appeared in both the 0 and 90° data of Ref. 19; on the other hand, the 0 and 90° data differ from each other by about 10% in the energy range covered. The absolute cross section was estimated to have an uncertainty of 20% in Ref. 20. However, near 12.4 MeV, the absolute cross section of Ref. 21 (which is also estimated as being correct to within 20%) is about 1.5 times the value given in Ref. 20.

Reibel and Mann[2] gave 4.6 ± 0.9 and 4.0 ± 0.8 mb at 6.9 and 7.1 MeV, respectively. These values are somewhat above our values as listed in Table III, but the disagreement may not be statistically significant. Our results are about a factor of 3 below the poor resolution results reported by Fuller and Hayward.[1] The poor resolution results of Tohei *et al.*,[3] after being corrected downward by the suggested[4] factor of 6, are rather close to the average value of our results, but the comparison of Cd and Bi scattering results[3,4] in these earlier experiments leave considerable uncertainty about the accuracy with which the correction factor is known.

Included in Tables II and III are the inferred total photon interaction cross sections, $\sigma_{\gamma t}$, and the related errors arising from only the statistical error in the elastic-scattering measurement. The information and assumptions that were used to obtain these total cross sections are described in Sec. IV. Equations (9)–(11) were used when no nucleon channels were open while Eqs. (13)–(16) were used when one proton channel was open. The details and reliability of the values of $\sigma_{\gamma t}$ are discussed in Sec. IV B. The last column in Tables II and III indicates what fraction of an electric dipole single-particle unit would have to be spread uniformly over a 1-MeV energy region to give the inferred photon interaction cross section, $\sigma_{\gamma t}$. The entries in the last column were derived using Eq. (5), which will be explained in Sec. IV.

TABLE III. Photon cross sections for Sn. See Sec. III for an explanation of the headings and entries in this table.

E_γ (MeV)	ΔE_γ (keV)	$\sigma_{\gamma\gamma}$ (mb) uncorrected	Assumed fraction of Sn contributing	$\sigma_{\gamma\gamma}$ corrected (mb)	$\sigma_{\gamma t}$ (mb)	Single-particle units per MeV
5.98	70	2.33	1.0	2.33 ± 0.64	4.6 ± 0.9	0.068
6.11	70	2.71	1.0	2.71 ± 0.66	5.3 ± 0.9	0.075
6.20	70	1.83	1.0	1.83 ± 0.59	4.2 ± 0.9	0.058
6.28	70	2.18	1.0	2.18 ± 0.62	4.9 ± 0.9	0.065
6.40	70	5.04	1.0	5.04 ± 0.86	9.0 ± 1.15	0.116
6.49	70	4.77	1.0	4.77 ± 0.76	8.9 ± 1.05	0.111
6.59	70	4.93	0.914	5.39 ± 0.83	10.0 ± 1.15	0.121
6.70	70	4.41	0.914	4.82 ± 0.87	9.6 ± 1.25	0.113
6.79	70	4.07	0.914	4.45 ± 0.87	9.4 ± 1.25	0.107
6.87	70	2.41	0.914	2.64 ± 0.57	6.8 ± 0.95	0.076
7.00	70	2.72	0.838	3.25 ± 0.61	8.2 ± 1.00	0.088
7.09	70	3.33	0.838	3.98 ± 0.71	9.6 ± 1.1	0.101
7.14	70	2.81	0.838	3.35 ± 0.48	8.8 ± 0.8	0.091
7.24	70	2.94	0.838	3.51 ± 0.52	9.4 ± 0.9	0.095
7.34	70	3.98	0.838	4.75 ± 0.57	12.2 ± 0.95	0.119
7.37	70	3.85	0.838	4.60 ± 0.73	11.9 ± 1.2	0.117
7.47	70	4.96	0.838	5.92 ± 0.79	15.0 ± 1.3	0.142
7.53	60	4.19	0.838	5.00 ± 1.09	13.3 ± 1.9	0.124
7.58	70	3.66	0.835	4.38 ± 1.09	12.4 ± 1.9	0.113
7.69	70	3.81	0.835	4.56 ± 0.65	13.4 ± 1.2	0.119
7.79	60	4.21	0.835	5.04 ± 0.62	14.8 ± 1.2	0.128
7.86	70	4.43	0.835	5.31 ± 0.66	15.7 ± 1.25	0.135
7.99	70	4.91	0.835	5.88 ± 0.64	17.7 ± 1.2	0.145
8.10	70	4.86	0.835	5.82 ± 0.59	18.4 ± 1.2	0.148
8.16	60	4.33	0.835	5.19 ± 0.71	17.4 ± 1.5	0.139
8.22	70	3.74	0.835	4.48 ± 0.55	16.5 ± 1.25	0.128
8.33	60	4.03	0.835	4.83 ± 0.63	18.0 ± 1.5	0.137
8.39	70	4.71	0.835	5.64 ± 0.63	20.1 ± 1.4	0.151
8.49	70	4.23	0.835	5.07 ± 0.72	20.0 ± 2.0	0.147
8.60	70	3.67	0.775	4.73 ± 0.81	20.1 ± 2.0	0.143
8.69	70	3.05	0.775	3.93 ± 0.75	18.9 ± 2.2	0.132
8.79	70	1.64	0.775	2.12 ± 0.55	13.8 ± 2.0	0.083
8.89	60	1.64	0.728	2.25 ± 0.65	15.1 ± 2.4	0.099
8.98	70	2.22	0.728	3.05 ± 0.53	18.8 ± 1.8	0.123
9.10	70	2.11	0.728	2.90 ± 0.60	19.1 ± 2.2	0.123
9.18	70	1.20	0.398	3.02 ± 0.90	19.6 ± 3.3	0.124
9.21	70	0.77	0.398	1.94 ± 1.00	15.8 ± 4.4	0.099
9.29	70	1.22	0.398	3.07 ± 1.00	21.1 ± 3.8	0.128
9.36	70	0.79	0.158	5.00 ± 2.32	30.1 ± 8.0	0.179

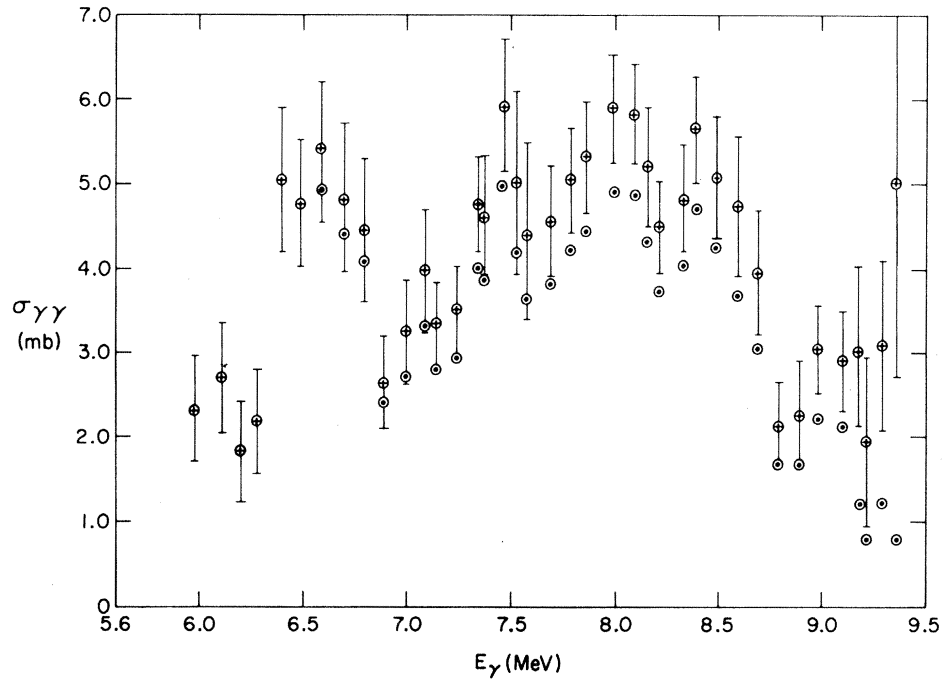

FIG. 2. The photon quasielastic-scattering cross section of Sn. The experimentally measured points are shown as circled dots without any indication of statistical error. The numerical values of these cross sections assume that all of the Sn isotopes have equal cross sections. The crosses represent the cross sections under the more reasonable assumption that only nuclei which are excited below their neutron threshold contribute to the scattering. Numerical values are given in Table III.

IV. DISCUSSION AND CONCLUSIONS

A. Relations Between the Average Cross Section and the Level Parameters

1. *General Effects of Width Variations*

The contribution of the ith nuclear level to the energy integrated elastic scattering is proportional to $\Gamma_{\gamma 0 i}{}^2/\Gamma_{t i}$, where $\Gamma_{\gamma 0 i}$ is the partial width for photon decay to the ground state, and $\Gamma_{t i}$ is the total level width. When the incident γ-ray resolution, ΔE, is much larger than the nuclear level spacing, D, the measured average elastic-scattering cross section includes contributions from $\Delta E/D = n$ levels,

$$\sigma_{\gamma\gamma} \propto \frac{1}{\Delta E}\sum_{i=1}^{n}\frac{\Gamma_{\gamma 0 i}{}^2}{\Gamma_{t i}} = \frac{n}{\Delta E}\,\frac{1}{n}\sum_{i=1}^{n}\frac{\Gamma_{\gamma 0 i}{}^2}{\Gamma_{t i}} \equiv \frac{1}{D}\langle \Gamma_{\gamma 0}{}^2/\Gamma_t\rangle . \tag{1}$$

For a zero-spin ground state and dipole excitation, the proportionality constant can be expressed numerically in terms of the excitation energy, E_γ,

$$\sigma_{\gamma\gamma} = 1.15\ \text{mb}\left(\frac{10\ \text{MeV}}{E_\gamma}\right)^2 \frac{10^5}{D}\langle \Gamma_{\gamma 0}{}^2/\Gamma_t\rangle . \tag{2}$$

The average of the total γ-ray interaction cross section, $\sigma_{\gamma t}$, has greater theoretical significance because it is directly related to the ground-state partial decay widths, $\Gamma_{\gamma 0 i}$; these widths, in turn, are proportional to the squares of the dipole matrix elements between the excited nuclear states and the ground state.

$$\sigma_{\gamma t} = 1.15\ \text{mb}\left(\frac{10\ \text{MeV}}{E_\gamma}\right)^2 \frac{10^5}{D}\langle \Gamma_{\gamma 0}\rangle . \tag{3}$$

The product of the energy interval and the average total cross section gives a direct measure of the sum of the partial ground-state decay widths for all of the levels in ΔE.

$$\sum_{i=1}^{n}\Gamma_{\gamma 0 i} = \frac{\sigma_{\gamma t}}{1.15\ \text{mb}} \times 10^{-5}\,\Delta E\left(\frac{E_\gamma}{10\ \text{MeV}}\right)^2 . \tag{4}$$

As a numerical illustration of Eq. (4), a cross section of 11.5 mb at 10 MeV implies 100 eV of ground-state transition width per MeV of excitation energy. For comparison, a Weisskopf-Moszkowski single-particle unit, which is proportional to $A^{2/3}$, has a value of $\Gamma_u = (1.36\ \text{keV})[E_\gamma/(10\ \text{MeV})]^3$ for ^{90}Zr (with R taken as $1.2A^{1/3}$ F). It is convenient to have the numerical relation between the summed partial widths and the single-particle unit, Γ_u:

$$\left(\frac{\sum_{i=1}^{n}\Gamma_{\gamma 0 i}}{\Gamma_u}\right)_{^{90}\text{Zr}} = \frac{\sigma_{\gamma t}\,\Delta E}{156\ \text{mb MeV}}\left(\frac{10\ \text{MeV}}{E_\gamma}\right), \tag{5a}$$

$$\left(\frac{\sum_{i=1}^{n}\Gamma_{\gamma 0 i}}{\Gamma_u}\right)_{^{120}\mathrm{Sn}} = \frac{\sigma_{\gamma t}\,\Delta E}{189\ \mathrm{mb\ MeV}}\left(\frac{10\ \mathrm{MeV}}{E_\gamma}\right), \quad (5b)$$

Equation (5) was used to obtain the entries in the last column of Tables II and III once $\sigma_{\gamma t}$ was determined. An entry of 0.14 single-particle units per MeV implies that the observed cross section would be expected if a 1-MeV interval contained 0.14 of the transition strength expected for a single-particle unit. If the corresponding average cross section is obtained for a 70-keV energy region, that region would have 0.01 single-particle units.

The relation between $\sigma_{\gamma t}$ and $\sigma_{\gamma\gamma}$ cannot be expressed in simple closed form, but $\sigma_{\gamma t}$ is an implicit function of $\sigma_{\gamma\gamma}$, and the ratio $\sigma_{\gamma t}/\sigma_{\gamma\gamma}$ is a slowly varying function of the unknown parameters in the problem. This ratio can be expressed in terms of average widths and average width ratios with the aid of Eqs. (2) and (3)

$$\frac{\sigma_{\gamma t}}{\sigma_{\gamma\gamma}} = \langle\Gamma_{\gamma 0}\rangle \Big/ \left\langle \frac{\Gamma_{\gamma 0}^{\,2}}{\Gamma_t}\right\rangle. \quad (6)$$

2. *No Open Nucleon Channels*

The evaluation of the right-hand side of Eq. (6) depends on the components of the total width of the ith level, Γ_{ti}. Below nucleon emission thresholds, the total width can probably be well represented as the sum of the ground-state partial width, $\Gamma_{\gamma 0 i}$, and a constant width, Γ_c, which is itself the sum of many partial widths for γ-ray decays to excited states,

$$\Gamma_{ti} = \Gamma_{\gamma 0 i} + \Gamma_c\,. \quad (7)$$

The cross-section ratio of Eq. (6) can be expressed conveniently in terms of an enhancement factor, E_1, whose value depends on the distribution of the partial widths, $\Gamma_{\gamma 0 i}$,

$$E = \left\langle \frac{\Gamma_{\gamma 0}^{\,2}}{\Gamma_t}\right\rangle \Big/ \frac{\langle\Gamma_{\gamma 0}\rangle^2}{\langle\Gamma_t\rangle}. \quad (8)$$

For any particular distribution, the enhancement in elastic scattering depends only on the ratio, $\Gamma_c/\langle\Gamma_{\gamma 0}\rangle \equiv c$. For a total width given by Eq. (7), and for a Porter-Thomas distribution of partial widths, E_1 has a value of 3 for very large values of c, and E_1 decreases to 1 as c becomes very small. The calculation of the enhancement factor is discussed in the Appendix [near Eq. (A18)], and numerical values are given in Table IV. With the aid of Eqs. (6) and (8), $\sigma_{\gamma t}/\sigma_{\gamma\gamma}$ can be expressed in terms of $c \equiv \Gamma_c/\langle\Gamma_{\gamma 0}\rangle$ and E_1 (which is a function of c).

$$\frac{\sigma_{\gamma t}}{\sigma_{\gamma\gamma}} = \frac{\langle\Gamma_{\gamma 0}\rangle + \Gamma_c}{E_1\langle\Gamma_{\gamma 0}\rangle} = \frac{1+c}{E_1}\,. \quad (9)$$

Thus, $\sigma_{\gamma t}$ could be inferred from a measurement of $\sigma_{\gamma\gamma}$ if c were known.

The scattering cross section can be used to obtain another unique function of c and E_1, if approximate values are available for the level spacing, D, and the constant part of the widths, Γ_c. The appropriate combination of parameters can be written with the aid of Eq. (2).

TABLE IV. Effect of width variations. The observed elastic scattering, with the aid of Eq. (10), determines the average width ratio listed in column 1. If $\Gamma_{\gamma 0}$ follows a Porter-Thomas distribution, the corresponding nuclear parameters are listed in columns 2, 3, and 4. On the other hand, if the partial ground-state widths were constant from level to level, the values in column 1 would imply the ratios listed in column 5.

	Porter-Thomas distribution			Constant widths
$\frac{1}{\Gamma_c}\left\langle\frac{\Gamma_{\gamma 0}^{\,2}}{\Gamma_{\gamma 0}+\Gamma_c}\right\rangle$	$\frac{\sigma_{\gamma t}}{\sigma_{\gamma\gamma}}$	$\frac{\Gamma_c}{\langle\Gamma_{\gamma 0}\rangle}$	E_1	$\frac{\sigma_{\gamma t}}{\sigma_{\gamma\gamma}} = 1+\frac{\Gamma_c}{\Gamma_{\gamma 0}}$
2.86×10^{-4}	34.97	100	2.888	59.6
1.67×10^{-3}	14.93	40	2.764	25.0
6.09×10^{-3}	8.22	20	2.556	13.3
1.02×10^{-2}	6.52	15	2.454	10.4
2.08×10^{-2}	4.81	10	2.286	7.45
3.04×10^{-2}	4.12	8	2.186	6.26
4.88×10^{-2}	3.41	6	2.050	5.05
9.27×10^{-2}	2.69	4	1.855	3.82
0.258	1.94	2	1.547	2.53
0.656	1.53	1	1.311	1.83
1.028	1.39	0.7	1.223	1.61
1.545	1.29	0.5	1.159	1.45
4.404	1.14	0.2	1.057	1.19
9.31	1.07	0.1	1.024	1.10

$$10^{-5}\frac{D}{\Gamma_c}\frac{\sigma_{\gamma\gamma}}{1.15\text{ mb}}\left(\frac{E_\gamma}{10\text{ MeV}}\right)^2=\frac{1}{\Gamma_c}\left\langle\frac{\Gamma_{\gamma 0}{}^2}{\Gamma_t}\right\rangle. \quad (10)$$

The dependence on c can be written simply by combining Eq. (8) with Eq. (10).

$$\frac{1}{\Gamma_c}\left\langle\frac{\Gamma_{\gamma 0}{}^2}{\Gamma_t}\right\rangle=\frac{E_1}{c(1+c)}. \quad (11)$$

From Eqs. (9)–(11), it is clear that $\sigma_{\gamma t}/\sigma_{\gamma\gamma}$ can be obtained from the combination $(D/\Gamma_c)\sigma_{\gamma\gamma}$; the sensitivity of $\sigma_{\gamma t}/\sigma_{\gamma\gamma}$ to the assumed value of D/Γ_c depends on how $(1+c)/E_1$ varies with the inferred value of $E_1/[c(1+c)]$. The values given in Table IV indicate that $\sigma_{\gamma t}/\sigma_{\gamma\gamma}$ can be obtained rather precisely below the nucleon emission threshold even if $\langle\Gamma_{\gamma 0}{}^2/\Gamma_t\rangle/\Gamma_c$ is uncertain due to uncertainties in D/Γ_c. The values of $\sigma_{\gamma t}/\sigma_{\gamma\gamma}$ and E_1 given in columns two and four of Table IV assume a Porter-Thomas width distribution; if the partial widths were assumed constant (i.e., if E_1 were assumed equal to 1), a larger value of $\sigma_{\gamma t}/\sigma_{\gamma\gamma}$ would be inferred, as shown in column five of Table IV.

When average cross sections are measured, corrections must sometimes be made for the resonant absorption of γ rays in the sample. The peak cross sections at resonances in the center-of-mass system are larger than the average cross section by a factor of $(2/\pi)(D/\langle\Gamma\rangle)$. However, the cross sections in the laboratory reference frame are Doppler broadened enough to reduce resonant absorption despite the effective enhancement in absorption caused by the variations of level widths.[8] As mentioned in Sec. II, resonant absorption effects in our samples are negligible.

3. *One Open Nucleon Channel*

The ^{90}Zr data can be interpreted if the analysis is generalized to include proton decay to a single final state; the total level width of Eq. (7) must be generalized to include a proton decay width, Γ_p.

$$\Gamma_{ti}=\Gamma_{\gamma 0i}+\Gamma_{pi}+\Gamma_c. \quad (12)$$

If the proton width follows a Porter-Thomas distribution, the average proton emission is less than would be expected if all levels had a constant proton width equal to the average width of the distribution, $\langle\Gamma_p\rangle$. Therefore, the elastic photon scattering would be more enhanced when the proton width follows a Porter-Thomas distribution as explained in the Appendix. The enhancement factor is defined in Eq. (8), but will be called E_2 in the following discussion to emphasize that it depends on $\langle\Gamma_p\rangle/\langle\Gamma_{\gamma 0}\rangle \equiv q^2$ as well as on $\Gamma_c/\langle\Gamma_{\gamma 0}\rangle \equiv c$; E_2 is written explicitly in Eq. (13a).

$$\frac{1}{\Gamma_c}\left\langle\frac{\Gamma_{\gamma 0}{}^2}{\Gamma_t}\right\rangle\equiv\frac{E_2}{\Gamma_c}\frac{\langle\Gamma_{\gamma 0}\rangle^2}{\langle\Gamma_{\gamma 0}\rangle+\langle\Gamma_p\rangle+\Gamma_c}. \quad (13a)$$

Inasmuch as the left side of Eq. (13a) is obtained from the experimental elastic-scattering cross section, as indicated in Eq. (10), this cross section determines the value of one function of the two parameters q^2 and c,

$$\frac{1}{\Gamma_c}\left\langle\frac{\Gamma_{\gamma 0}{}^2}{\Gamma_t}\right\rangle=\frac{E_2(q^2,\,c)}{c(1+q^2+c)}\equiv R_1. \quad (13b)$$

The photoproton cross section can be used to obtain a different function of these same two parameters. The average of width ratios determined by the photoproton cross section can be obtained by analogy with Eq. (10).

$$10^{-5}\frac{D}{\Gamma_c}\left(\frac{\sigma_{\gamma p}}{1.15\text{ mb}}\right)\left(\frac{E_\gamma}{10\text{ MeV}}\right)^2=\frac{1}{\Gamma_c}\left\langle\frac{\Gamma_{\gamma 0}\Gamma_p}{\Gamma_t}\right\rangle. \quad (14)$$

The average on the right-hand side of Eq. (14) is less than the corresponding ratio of average widths by a reduction factor F, defined by Eq. (15a).

$$\frac{1}{\Gamma_c}\left\langle\frac{\Gamma_{\gamma 0}\Gamma_p}{\Gamma_t}\right\rangle\equiv\frac{F}{\Gamma_c}\frac{\langle\Gamma_{\gamma 0}\rangle\langle\Gamma_p\rangle}{\langle\Gamma_{\gamma 0}\rangle+\langle\Gamma_p\rangle+\Gamma_c}. \quad (15a)$$

Because the reduction factor, F, depends on q^2 and c, the photoproton cross section determines the function R_2 defined in Eq. (15b),

$$\frac{1}{\Gamma_c}\left\langle\frac{\Gamma_{\gamma 0}\Gamma_p}{\Gamma_t}\right\rangle=F(q^2,\,c)\frac{q^2}{c(1+q^2+c)}\equiv R_2. \quad (15b)$$

The total photon interaction cross section can be expressed in terms of the enhancement and reduction factors with the aid of Eqs. (2), (3), and (13)–(15).

$$R_3\equiv\frac{\sigma_{\gamma\gamma}+\sigma_{\gamma p}}{\sigma_{\gamma t}}=\frac{E_2+Fq^2}{1+q^2+c}=c(R_1+R_2), \quad (16a)$$

$$\sigma_{\gamma t}=\frac{\sigma_{\gamma\gamma}+\sigma_{\gamma p}}{c(R_1+R_2)}=\frac{\sigma_{\gamma\gamma}+\sigma_{\gamma p}}{R_3}. \quad (16b)$$

Equations (13)–(16) are valid for any distribution of widths provided only that the total level width has no more than the three components specified in Eq. (12). If the photon and proton widths were constant from level to level, there would not be any enhancement or reduction, i.e., both E_2 and F would be equal to 1. If the photon widths vary from level to level, E_2 is greater than 1. If the proton widths are uncorrelated with the photon widths, F would be less than one; if the widths were completely correlated, F would be equal to E_2. The correlations can be described in terms of the variables x and y discussed in Appendix A near Eqs. (A6)–(A8); widths are uncorrelated if y and x are independent, while they are completely correlated if y is a constant times x, $y=Q^2x$. The dependence of E_2 and F on q^2 and c is governed by the distribution function.

The numerical values corresponding to two uncorrelated Porter-Thomas distributions are given in the Appendix. Table VIII gives the values of E_2/F; Table IX gives the values of R_1, R_2, and R_3. The numerical values indicate that R_3 is a slowly varying function, which indicates that $\sigma_{\gamma t}$ can be inferred relatively precisely even if c or R_1 or R_2 is not known very well. Thus, the measured values of elastic scattering and photoproton cross sections are used, with an assumed value of D/Γ_c to obtain R_1 and R_2 [using Eqs. (10), (13)–(15)]. These values of R_1 and R_2 are used to obtain R_3 with the aid of the numerical values in Table IX.

If the measured elastic scattering and photoproton cross sections were assumed to come from completely correlated widths, the ratio of the photoproton to the elastic scattering cross section would be equal to the ratio of the proton width to the photon width. For correlated widths,

$$Q^2 \equiv \frac{\sigma_{\gamma p}}{\sigma_{\gamma\gamma}} = \frac{\langle \Gamma_p \rangle}{\langle \Gamma_{\gamma 0} \rangle} . \tag{17}$$

In this case the analog of Eqs. (10) and (14) is

$$10^{-5} D \left(\frac{1+Q^2}{\Gamma_c}\right) \frac{(\sigma_{\gamma p}+\sigma_{\gamma\gamma})}{(1.15\ \text{mb})} \left(\frac{E_\gamma}{10\ \text{MeV}}\right)^2 = \frac{1+Q^2}{\Gamma_c} \left\langle \frac{\Gamma_{\gamma 0}(\Gamma_{\gamma 0}+\Gamma_p)}{\Gamma_{\gamma 0}+\Gamma_p+\Gamma_c} \right\rangle , \tag{18a}$$

$$= \frac{1+Q^2}{\Gamma_c} \left\langle \frac{\Gamma_{\gamma 0}^2(1+Q^2)}{(1+Q^2)\Gamma_{\gamma 0}+\Gamma_c} \right\rangle , \tag{18b}$$

$$= \frac{1}{\Gamma_c'} \left\langle \frac{\Gamma_{\gamma 0}^2}{\Gamma_{\gamma 0}+\Gamma_c'} \right\rangle , \tag{18c}$$

where $\Gamma_c' \equiv \Gamma_c/(1+Q^2)$. The right-hand side of Eq. (18c) can be used to enter Table IV and determine the enhancement factor, E_1, which in this case favors both elastic scattering and photoproton emission equally. [The value in column three of Table IV would be interpreted as $\Gamma_c'/\Gamma_{\gamma 0} = \Gamma_c/(\Gamma_p+\Gamma_{\gamma 0})$; the value in column two of Table IV would be interpreted as $\sigma_{\gamma t}/(\sigma_{\gamma\gamma}+\sigma_{\gamma p})$.]

The net effect of assuming completely correlated widths would be to increase the inferred value of $\sigma_{\gamma t}$ because the inferred inelastic γ-ray scattering would be increased. For the ^{90}Zr data, the inferred inelastic scattering is relatively small for uncorrelated widths, and hence the effect of correlations is to increase the inferred interaction cross section by about 6%. Thus, the main effect of assuming correlated widths would be to reduce the inferred value of $\langle \Gamma_p \rangle / \langle \Gamma_{\gamma 0} \rangle$ considerably. The inferred value of $\langle \Gamma_p \rangle / \langle \Gamma_{\gamma 0} \rangle$ would be only $\sigma_{\gamma p}/\sigma_{\gamma\gamma}$ if there were complete width correlations; with no correlations $\langle \Gamma_p \rangle / \langle \Gamma_{\gamma 0} \rangle = (E_2/F)(\sigma_{\gamma p}/\sigma_{\gamma\gamma})$, as can be shown from Eqs. (10), (13)–(15).

B. Total Cross Sections and Level Parameters

1. Sn *Cross Section and Parameters*

The values of the combination of parameters, $(1/D)\langle \Gamma_{\gamma 0}^2/\Gamma_t \rangle$, can be obtained directly from the elastic-scattering cross section with the aid of Eq. (2); typical values are listed in column three of Table V. The total interaction cross section can be obtained from Eqs. (9)–(11) if the level spacing $D(E)$, and the constant part of the level width, Γ_c are known. Neutron resonance studies often provide a good estimate both of Γ_c and of the level spacing, $D(E_B)$, at the neutron binding energy, E_B. The level spacing at other energies is calculated using a nuclear temperature inferred from the energy distribution of nucleons emitted statistically in other nuclear reactions.

In the region of the Periodic Table near Sn, the total γ-ray widths are about equal to 0.1 eV; we therefore set $\Gamma_c = 0.1$ eV. The values of D required in Eq. (9) were obtained from measured values[24] near 9.2 MeV in ^{116}Sn, ^{118}Sn, and ^{120}Sn, together with an assumed constant nuclear temperature. The level spacing of 1^- states, D, was chosen as 40 eV at 9.2 MeV to correspond to the observed[24] 30-eV spacing for a mixture of 0^- and 1^- states just above the neutron threshold of ^{120}Sn. (The spacings in ^{116}Sn and ^{118}Sn are consistent with this.) The energy dependence of the level spacing was taken as $D(E) = D(9.2\ \text{MeV})\exp[(9.2-E)/T]$. The temperature was taken as $T = 0.73$ from the level density formula and the parameters given by Gil-

TABLE V. Typical level parameters for Sn.

Energy (MeV)	$\sigma_{\gamma\gamma}$ (mb)	$\frac{10^5}{D}\left\langle \frac{\Gamma_{\gamma 0}^2}{\Gamma_t} \right\rangle$	$10^{-5}\frac{D}{\Gamma_c}$ [a]	$\left\langle \frac{\Gamma_{\gamma 0}^2}{\Gamma_c \Gamma_t} \right\rangle$	$\sigma_{\gamma t}$ (mb)	$\langle \Gamma_{\gamma 0} \rangle$ (meV)
6.2	2	0.67	0.25	0.16	4.5	35
6.5	5	1.8	0.17	0.30	9.2	55
7.8	5	2.6	0.027	0.072	14.8	20
8.5	5.5	3.5	0.010	0.036	21.1	14
8.8	2.2	1.5	0.007	0.01	14.2	6.8

[a] Assuming $\Gamma_c = 0.1$ eV, $D(9.2\ \text{MeV}) = 40$ eV, and $T = 0.73$ MeV.

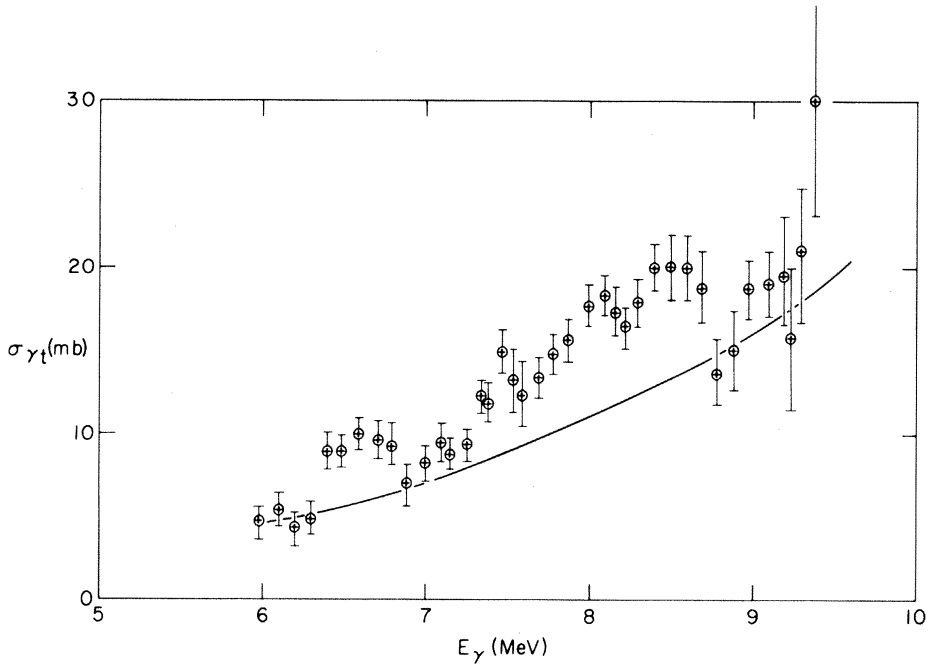

FIG. 3. The total photon interaction cross section of Sn. It was assumed that only those isotopes contribute which have photoneutron thresholds above the γ-ray energy. It was also assumed that all contributing isotopes have equal cross sections. The photon partial widths are assumed to follow a Porter-Thomas distribution. The solid line represents the extrapolation of the Lorentz line which fits the photoneutron cross section in the region of the giant resonance as given in Ref. 27.

bert and Cameron.[25] Some effects of a lower temperature will be illustrated below because somewhat lower temperatures are implied by neutron spectra[26] associated with lower excitation energies of neighboring nuclei.

The values of D/Γ_c, such as are shown in column four of Table V, make it possible to obtain $\langle\Gamma_{\gamma 0}{}^2/\Gamma_t\rangle/\Gamma_c$, which with the aid of Table IV specifies $\sigma_{\gamma t}/\sigma_{\gamma\gamma}$. This ratio, combined with the measured scattering, provides the value of $\sigma_{\gamma t}$. The most precise determination of the average partial width $\langle\Gamma_{\gamma 0}\rangle$ can be made using Eq. (3) and the assumed value of D. In the entire energy range studied in the Sn experiment, the ratio $\sigma_{\gamma t}/\sigma_{\gamma\gamma}$ increased by a factor of less than 5 (i.e., from 1.79 to 8.8); as can be seen from Table IV, this corresponds to a decrease of $\Gamma_{\gamma 0}/\Gamma_c$ from about 0.6 to about 0.05 (i.e., $\Gamma_{\gamma 0}$ decreases from about 60 mV at 6.4 MeV to about 4.7 mV at 9.21 MeV). Between 6.4 and 9.21 MeV, the total cross section increases from 9 to 15.8 mb (a factor of 1.75) while $\langle\Gamma_{\gamma 0}\rangle/D$ increases by about 3.5. The major decrease in $\langle\Gamma_{\gamma 0}\rangle$ is dominated by the decrease in D (by a factor of 47). Over the larger energy range from 6.2 to 9.29 MeV, the interaction cross section increases by a factor of 5, $\langle\Gamma_{\gamma 0}\rangle/D$ increases by a factor of 11, and D decreases by a factor of 71.

The inferred values of $\sigma_{\gamma t}$ depend on the assumed value D/Γ_c, but not very sensitively. Table VI presents some examples of the effects of changing D.

TABLE VI. Sensitivity of Sn level parameters to D and T.

D(9.2 MeV) / T	40 eV / 0.73 MeV		80 eV / 0.73 MeV		40 eV / 0.63 MeV		Extrapolated[a] from giant resonance
E (MeV)	$\sigma_{\gamma t}$ (mb)	$\langle\Gamma_{\gamma 0}\rangle$ (meV)	$\sigma_{\gamma t}$ (mb)	$\langle\Gamma_{\gamma 0}\rangle$ (meV)	$\sigma_{\gamma t}$ (mb)	$\langle\Gamma_{\gamma 0}\rangle$ (meV)	$\sigma_{\gamma t}$ (mb)
6.2	4.5	35	3.5	62	3.6	58	5.0
6.5	9.2	55	7.8	90	8.0	84	5.8
7.8	14.8	20	11.7	35	13.2	25	10.0
8.5	21.1	14	16.3	20	20.0	15	13.3
8.8	14.2	6.8	10.6	9.8	13.8	7.2	16.0

[a]From data given in Ref. 27.

Increasing D by a factor of 2 lowers the inferred total cross section by about 20%, and raises the inferred value of $\langle\Gamma_{\gamma 0}\rangle$ by about 60%. The last column in Table VI gives the photon interaction cross section implied by the average resonance parameters[27] for ^{116}Sn, ^{118}Sn, and ^{120}Sn: $E_R = 15.56$ MeV, $\sigma_{peak} = 267$ mb, and $\Gamma = 4.6$ MeV. This extrapolated cross section is shown by the solid line in Fig. 3.

Over most of the energy range, our inferred total cross sections (in Fig. 3) are about 50% higher than these extrapolated values. This excess of cross section is not inconsistent with the low-energy portions of the photoneutron cross sections[27] which are also high for ^{118}Sn, ^{120}Sn, and ^{124}Sn. (There is some variation in the giant resonance parameters from isotope to isotope. The largest low-energy cross section would be predicted by the parameters for ^{120}Sn which are: $E_R = 15.4$ MeV, $\sigma_{peak} = 280$ mb, and $\Gamma = 4.88$ MeV. In the energy range shown in Fig. 3, these parameters would predict cross sections about 21% higher than those shown by the solid curve. However, ^{120}Sn is only 33% of natural Sn, and the expected average extrapolated cross section for the contributing isotopes is close to the solid curve of Fig. 3.)

The observed elastic scattering is almost surely dominated by the three most abundant isotopes ^{116}Sn, ^{118}Sn, and ^{120}Sn. Although the total cross sections listed in Table III assume for simplicity that all Sn isotopes have equal cross sections, it is quite likely that the odd Sn isotopes, with their smaller level spacings, contribute disproportionately little to elastic scattering.[12] For this reason the cross sections listed from 5.98 to 6.49 MeV might require a correction by a factor of about 1.2, and those from 6.59 to 6.87 MeV might require a correction of 1.08.

The poor resolution of the γ-ray detector makes it impossible to know whether some inelastic scattering is included in the measured quasielastic scattering, but the net effect of any inelastic scattering would almost surely be quite small. The energy dependence[8] of photon widths would imply that the partial width for decay to the first excited 2^+ state at about 1.1 or 1.2 MeV in even Sn isotopes would be only one half as big as the ground-state partial width. If the widths to the excited and ground state were uncorrelated, the inelastic scattering to the first excited state would be only about 19% of the elastic scattering. Even though the inelastic scattering would not have been resolved, the detection equipment would have discriminated against it. In view of these experimental conditions it would be surprising indeed if less than 90% of the observed quasielatic scattering were due to elastic scattering; if only 90% of the observed scattering were elastic, the total cross section would be about 95% of the values listed in Table III.

2. *Photon Interaction Cross Section and Level Parameters for* ^{90}Zr

The total photon interaction cross section can be inferred from the observed scattering at energies below 10.5 MeV because photoproton emission is negligible. Above 10.5 MeV, the scattering and photoproton results must be combined. In either case, it is necessary to assume values of D/Γ_c in order to determine the total cross section. In addition, the partial widths are assumed to follow a Porter-Thomas distribution.

In the neighborhood of ^{90}Zr, isotopes reached by slow neutrons have total radiation widths[28,29] which are within a factor of 2 of 0.2 eV; we therefore use $\Gamma_c = 0.2$ eV. There are no reliable direct level spacing data for ^{90}Zr, and there is no obvious way to infer the ^{90}Zr level spacing with confidence from experimentally determined spacings in neighboring nuclei. We used a nuclear temperature of $T = 1.19$ MeV as suggested by Gilbert and Cameron,[25] but estimated the level spacing to be 8 times larger than given by the parameters of Gilbert and Cameron. Our estimate of the level spacing is 2 keV at 9-MeV excitation and 160 eV at 12-MeV excitation.

In this paragraph we shall briefly present the considerations on which our estimate of level spacing is based; these are presented to indicate the large uncertainty that exists. First, the level density parameters of Gilbert and Cameron[25] do not reflect the exceptionally tight binding of the ^{90}Zr ground state; the probable inaccuracy of the proposed parameters for closed-shell nuclei had been recognized.[25] An estimate of how much larger D should be for ^{90}Zr was obtained from available data on neighboring nuclei. For example, the spacing of spin $\frac{1}{2}$ states in ^{91}Zr at 7.2 MeV had been measured[30] to be about 4.5 keV; assuming that the level density is proportional to the spin factor, $2I+1$, implies $D = 3$ keV for 1^- states. A weak coupling model would imply that the level density in ^{91}Zr would be more than five times that in ^{90}Zr. This reasoning implies that the level spacing in ^{90}Zr near 7.2 MeV would be greater than 15 keV, which is 12 times the spacing predicted by the Gilbert-Cameron parameters. This greater spacing is still a factor of 10 lower than would be implied if the ^{89}Y(^{3}He, d)^{90}Zr experiment[31] had indeed identified all of the 2^- states; on the other hand, some 2^- states with weak single-particle components could have been missed. Another source of information is the observed level spacing near 9 MeV in ^{96}Mo and ^{98}Mo. These data[29,32] imply a spacing of 1^- states of 500 eV; allowing for the more tightly bound ground state of ^{90}Zr, the same spacing

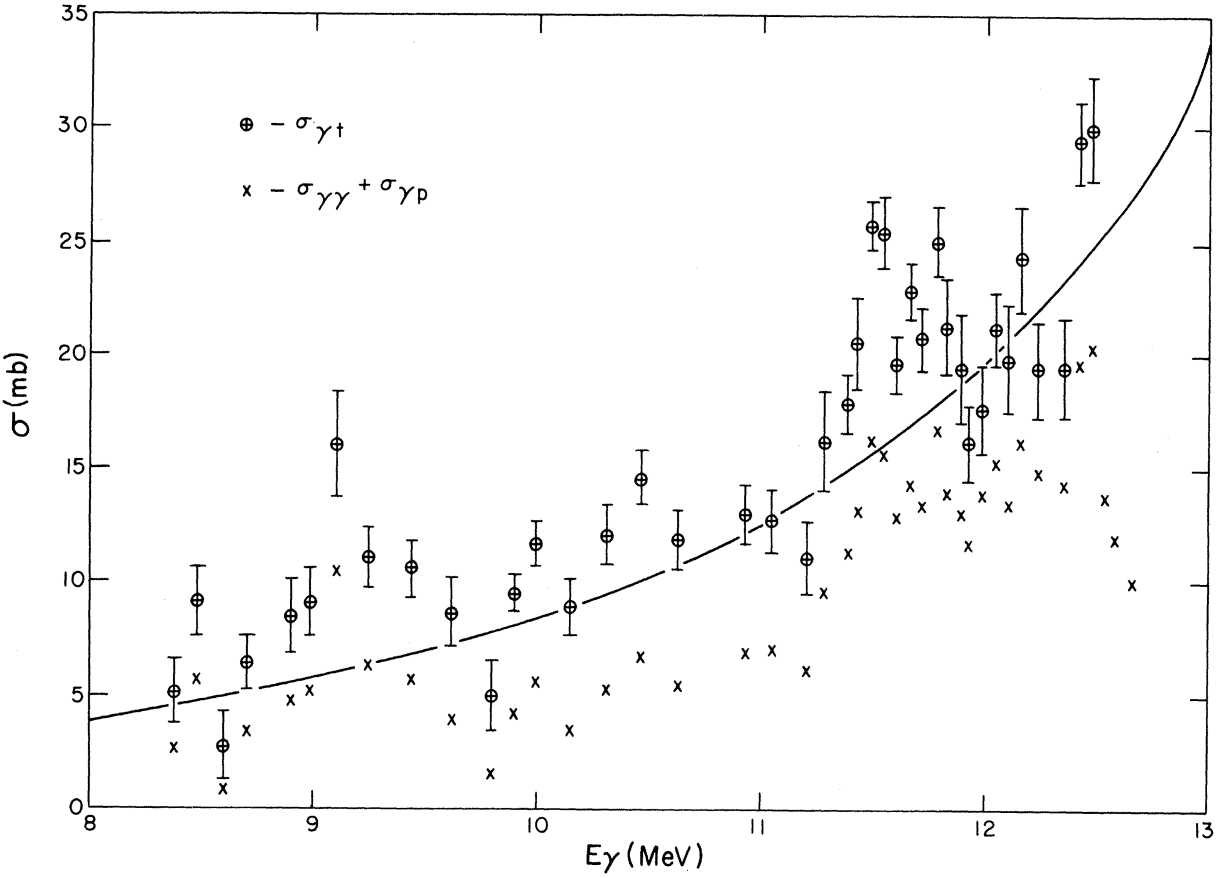

FIG. 4. The photon interaction cross section of ^{90}Zr. It was assumed that the elastic photon scattering above 8.68 MeV was due to ^{90}Zr. The inferred cross sections are shown by the circled crosses with experimental errors corresponding to the statistical uncertainty in only the elastic-scattering cross section. Below 10.62 MeV, the measured photon scattering cross section is shown by the diagonal crosses; at and above the 10.62 MeV the diagonal crosses represent the sum of the elastic scattering and photoproton cross sections inferred from the data in Refs. 19 and 20. The line is the low-energy extrapolation of the Lorentz line which matches the photoneutron cross section of ^{90}Zr in the giant resonance region according to Ref. 13.

might be expected in ^{90}Zr at a higher energy, such as 10 MeV. A spacing of 500 eV at 10 MeV is five times larger than that predicted by the Gilbert-Cameron parameters.

The inferred total interaction cross sections are shown in Table II and Fig. 4, assuming the values $\Gamma_c = 0.2$ eV, $D(12\text{ MeV}) = 160$ eV, and $T = 1.19$ MeV. The errors shown in the total cross section reflect only the statistical error in the measured scattering. The statistical errors associated with the photoproton cross section should be negligibly small above 11.95 MeV, where the indicated cross sections are 100-keV averages of data obtained with high statistical accuracy and 10-keV resolution[20]; the statistical errors in the lower-energy photoproton data[19] are also probably negligible. No allowance has been made for the estimated[20] absolute error of about 20% in the photoproton cross section.

The inferred total cross sections are relatively insensitive to errors in the assumed values of D/Γ_c. In the energy range from 8.38 to 10.46 MeV, the ratio of $\sigma_{\gamma t}/\sigma_{\gamma\gamma}$ varies by only a factor of 2; it has a minimum value of 1.49 at 9.09 MeV and a maximum value of 2.96 at 9.79 MeV. The values in Table IV indicate that $\sigma_{\gamma t}/\sigma_{\gamma\gamma}$ is relatively insensitive to D/Γ_c (i.e., to $\langle\Gamma_{\gamma 0}{}^2/\Gamma_t\rangle/\Gamma_c$) in this range of values. For example, if D/Γ_c were a factor of 2 smaller at 9.09, 9.24, and 10.31 MeV the inferred total cross sections would increase by 18, 23, and 26%; if D/Γ_c were a factor of 2 larger, the inferred total cross sections at the same energies would decrease by 13, 16, and 20%. The total cross sections are equally insensitive to D/Γ_c at energies where photoproton emission is observed. This insensitivity is implied by the entries in Table IX in the Appendix, in which it can be seen that $R_3 \equiv (\sigma_{\gamma\gamma} + \sigma_{\gamma p})/\sigma_{\gamma t}$ is a slowly varying function of R_1 and R_2 [of Eqs. (13) and (15)] when $\sigma_{\gamma\gamma}/\sigma_{\gamma p} = R_1/R_2$ is not changed. For example, at 11.42, 11.49, and

12.23 MeV, decreasing D/Γ_c by a factor of 2 would increase $\sigma_{\gamma t}$ by 21, 22, and 24%; increasing D/Γ_c by a factor of 2 at these energies would decrease $\sigma_{\gamma t}$ by only 18, 13, and 9%, respectively.

The total interaction cross sections above 10.6 MeV were calculated assuming that the proton and photon widths of the levels are completely uncorrelated. However, the total interaction cross sections are very insensitive to this assumption; if these widths were completely correlated the inferred total cross sections would increase by only 7% or less. (The main effect of correlations, as mentioned in Sec. IV A3, is to change the inferred values of $\Gamma_p/\Gamma_{\gamma 0}$; this does not influence the inferred values of inelastic γ-ray scattering. The effects of correlations will be discussed in Sec. IV C3.)

Neutron emission is assumed to be negligible until neutrons can reach the isomeric level at 0.59 MeV in ^{89}Zr. From the threshold for ground-state neutron emission at about 11.96 to about 12.55 MeV, the transmission[33] of f-wave neutrons is less than 0.015; the s-wave proton transmission is about one order of magnitude higher.[33] On the other hand, above 12.55 MeV, the photoneutron cross section would be important, and the total photon interaction cross section cannot be determined without it.

The solid line shown in Fig. 4 represents the cross section predicted by the parameters[13] which fit the giant resonance of ^{90}Zr. The observed average cross section is about 40% higher than the extrapolated value.

C. Conclusions and Summary

1. *Intermediate Structure*

It is clear from Figs. 3 and 4 that the photon interaction cross section does not simply increase smoothly with energy. There are at least several statistically significant rapid variations which correspond to concentrations of strength. The most obvious examples can be found between 11.2 and 11.8 MeV in ^{90}Zr. The cross section rises by a factor of 2 between 11.2 and 11.5 MeV. The inferred drop in the cross section above 11.8 MeV is almost surely a feature of the total interaction cross section rather than a manifestation of the neutron threshold.

The cross section for the mixture of Sn isotopes in Fig. 3 also contains rapid variations with energy which strongly suggest strength concentrations. For example, the cross section rises by about 80% near 6.4 MeV. The abrupt 30% decrease in cross section between 8.6 and 8.8 MeV indicates a decrease in the interaction cross section for at least some of the most abundant isotopes; so large an effect could not be attributed to the onset of neutron emission from ^{122}Sn which has an abundance of only 4.7%. Inasmuch as the data represent an average over several isotopes, Fig. 3 should be considered as representing a lower limit to the variations that might exist in the cross sections of individual isotopes.

A concentration of photon strength in ^{90}Zr near 12 MeV had been inferred earlier[19] from proton capture γ-ray data. The dominant features of this averaged (p,γ_0) cross section are the monotonic rise of the average cross section from 2.2 to 4.2 MeV, followed by an abrupt drop (by a factor of 2) just above 4.2 MeV. Superimposed on this trend are more localized variations of less than 20%. The average (p,γ_0) cross section does not, by itself, indicate a concentration of photon strength because if uncorrelated photon and proton widths are assumed, the rising part of the (p,γ_0) cross section is just what would be expected from a quite smooth photon interaction cross section. Photoproton emission grows slowly, despite the rapidly increasing proton transmission coefficients, because of the enhancement in elastic scattering discussed in Sec. IV A and in the Appendix. For example, if the photon interaction cross section were given by the extrapolation of the giant resonance parameters and if the proton transmission coefficients were given by an optical model,[33] the ratio of proton to γ-ray width would be about 0.25, 2.5, 8.4, and 26 at 10.5, 11, 11.5, and 12 MeV; in the absence of correlations, the ratio of photoproton to elastic scattering at these same energies would be only 0.1, 0.7, 1.7, and 3.3. Thus, the observed slow increase in the (p,γ_0) cross section can be interpreted as due to a combination of the smoothly increasing photon interaction and the proton emission competition that would be expected in the absence of width correlations. The drop in the photoproton cross section just above a proton energy of 4.2 MeV can be explained by neutron competition rather than by a decrease in the photon interaction cross section. Thus, the increase in the photon interaction cross section shown in Fig. 4 near 11.5 MeV cannot be inferred on the basis of the photoproton cross section alone, but is established by the combination of photon scattering and photoproton data.

The cross sections in Figs. 3 and 4 make it clear that the photon transition strength is more localized than had been assumed. It will be difficult to obtain additional information about Sn until separated isotopes are obtained and inelastic γ-ray scattering measurements can be made. The availability of both photoproton and scattering data for ^{90}Zr make it a more promising example, as will be discussed in Sec. IV C3.

2. *Mechanism of Photon Interactions Below the Giant Resonance*

Both the magnitude of the average cross sections and the newly observed rapid variations give clues about the photon interaction mechanism. The entries in the last columns of Tables II and III, which were obtained from the total cross sections with the aid of Eq. (5), indicate that these cross sections correspond to the presence of about 0.1 single-particle electric dipole unit per MeV of excitation. These cross sections are large enough to indicate that electric dipole interactions must dominate in most of the studied energy range. For example, it would require seven single-particle magnetic dipole units to equal the width of 0.1 electric dipole unit. If there were a magnetic dipole giant resonance which concentrated seven single-particle magnetic dipole units in a 1-MeV interval, this magnetic dipole resonance could explain the observed cross section in only a 1-MeV region. By similar reasoning one can eliminate an important role for $E2$ transitions because the cross section attributable to 0.1 electric dipole units would require about 41 electric quadrupole single-particle units near 10 MeV of excitation. These arguments do not exclude the possibility of $M1$ or $E2$ transitions contributing either a small amount at all energies or a significant fraction at some particular energy. However, most of the observed cross section must be dominated by the electric dipole interaction.

Although the magnitude of the cross section is large enough to imply the electric dipole character of the interaction, it is too small to provide significant clues about the nuclear configurations that are responsible. For ^{90}Zr, the total cross sections in Fig. 4 vary from about 3 to 14% of the peak cross section in the giant resonance; for Sn, the cross sections of Fig. 3 vary from 2 to 8% of the peak cross section. Until a much more reliable theory of giant resonance damping becomes available, one cannot use the magnitude of this low-energy cross section to either confirm or reject the possibility that the same linear combination of particle-hole states which dominates the giant resonance also dominates this low-energy region. Thus, the cross section we observe might contain clues about the giant resonance configuration and the excitation energy range over which it spreads.

An alternate explanation of electric dipole transition strength near 8 MeV might be based on the residual strength which is left near 8 MeV after most of the transition probability is shifted upward in energy to form the giant resonance. Any independent particle model that is not too different from the harmonic oscillator would predict that most of the classical electric dipole sum of transition strength would be found near 8 MeV. Because the classical dipole sum corresponds to about 11 single-particle units (evaluated at 8 MeV), about 2 or 3 units would be expected in each 1-MeV interval near 8 MeV.

(The conventional electric dipole single-particle unit is about four times larger than the width expected for a favored single-nucleon transition because the effective charge of a nucleon for electric dipole transitions is actually about $e/2$, while the unrealistically large charge, e, was used to define the unit. For this reason, the 11 single-particle units correspond to about 44 favored single-nucleon transitions.)

The existence of the giant resonance near 16 MeV makes it clear that most of the dipole strength predicted near 8 MeV by an independent particle model is shifted upward in energy, presumably due to a residual particle-hole interaction. However, the quantitative details of the main shift in transition strength are still uncertain, and calculations will have to be improved considerably before they can reliably predict whether 0.1 single-particle unit per MeV remains in the unshifted particle-hole configurations.

These arguments make it clear that a determination of the magnitude of the cross section near 8 or 10 MeV is not sufficient to identify the nuclear configurations. The detailed energy dependence might provide clues. If the transition strength at low energies has contributions from different combinations of particle-hole configurations, the cross section might have local maxima and minima such as our data show. The local maxima suggest the presence of different particle-hole configurations. However, this conclusion must remain tentative until several configurations are identified with the aid of other partial cross sections.

The proton capture γ rays which lead to excited states in ^{90}Zr were interpreted[20] as evidence for the admixture of two-particle–two-hole states in the giant resonance. This interpretation was based on the assumptions[20] that only s-wave protons participated, and that the emission of high-energy γ rays is due to a quasidirect process dominated by the giant dipole resonance and occurring in a region of overlapping nuclear levels. However, protons with energies near 3 MeV can be captured in p waves and d waves, as well as in s waves. Therefore, the compound system formed by protons incident on ^{89}Y contains spins of 0^+, 1^+, 2^+, 2^-, and 3^- in addition to the spins 0^- and 1^- considered[20] in inferring the two-particle–two-hole mixtures. Furthermore, there is no reason to believe that levels of the same spin and parity overlap. At energies below the neutron emission threshold, the ratio of total level width, Γ_t, to level spacing, D, is less than 0.02, even for levels which can emit s-wave

protons. It therefore appears that the high-energy γ rays emitted following proton capture by ^{89}Y do not have any interpretable relation to the structure of the ^{90}Zr giant dipole resonance, and that the conclusions drawn[20] are unwarranted.

3. *Correlations of Photon and Proton Widths*

Accurate values of the elastic scattering and photoproton cross sections could provide information about width correlations if the proton strength function, Γ_p/D, were known from independent measurements. Quantitative conclusions about correlations would be premature at this time because the cross sections and the proton strength function are not yet well enough determined. However, in order to illustrate the exciting new information that can be obtained, the remainder of this section will explain the inferences that can be drawn when better data become available; for this purpose, the cross sections will be used as though they had negligible experimental error.

The combination of the elastic scattering and photoproton cross sections determine the total photon interaction and hence the photon strength function, $\Gamma_{\gamma 0}/D$, essentially independent of the width correlations. However, the degree of correlation strongly affects the inferred value of $\langle\Gamma_p\rangle/\langle\Gamma_{\gamma 0}\rangle$, and hence of $\langle\Gamma_{p0}\rangle/D$. For example, in the energy region from 10.6 to 11.6 MeV, an assumption of uncorrelated widths implies a value of $\langle\Gamma_p\rangle/\langle\Gamma_{\gamma 0}\rangle$ which is about 3 or 4 times larger than would follow from the assumption of correlated widths; the factor is close to 10 near 12 MeV. The inferred values of Γ_p/D are shown in Fig. 5; the circled crosses correspond to uncorrelated widths and the diagonal crosses correspond to correlated widths.

The degree of correlation could be inferred from the data of Fig. 5 if the true value of the proton strength function were known. As a guide about the energy dependence expected for Γ_p/D, Fig. 5 includes as a solid line the value of $\langle\Gamma_p\rangle/D$ calculated with the average parameters of the optical model derived at Los Alamos.[33] The contribution to Γ_p/D from protons of angular momentum j depends on the transmission coefficient T_j; $(\langle\Gamma_p\rangle/D)_j = T_j/2\pi$. However, relatively little is known experimentally about the value of the proton transmission coefficient at low energy, and it would be naive to assume that average optical-model parameters chosen to match high-energy scattering would give correct low-energy transmission coefficients. It would be much more desirable to obtain precise direct measurements of the proton interaction cross sections such as those recently reported[34] for Sn isotopes. Until these measurements are made, the comparison of photon scattering and photoproton cross sections together with the assumption of negligible width correlations might provide the best available estimate of the proton strength function.

In the absence of independent values of $\langle\Gamma_p\rangle/D$, one is forced to base conclusions about width correlations on the energy dependence of $\langle\Gamma_p\rangle/D$. In contrast with the concentration of photon strength function between 11.2 and 11.8 MeV, as seen in Fig. 4, the proton strength function exhibits no special features in this energy region. It therefore seems unlikely that the concentrated photon strength corresponds to a nuclear configuration which is related to proton emission. The inferred proton strength function would vary much more rapidly near 11.5 MeV if the extra photon strength

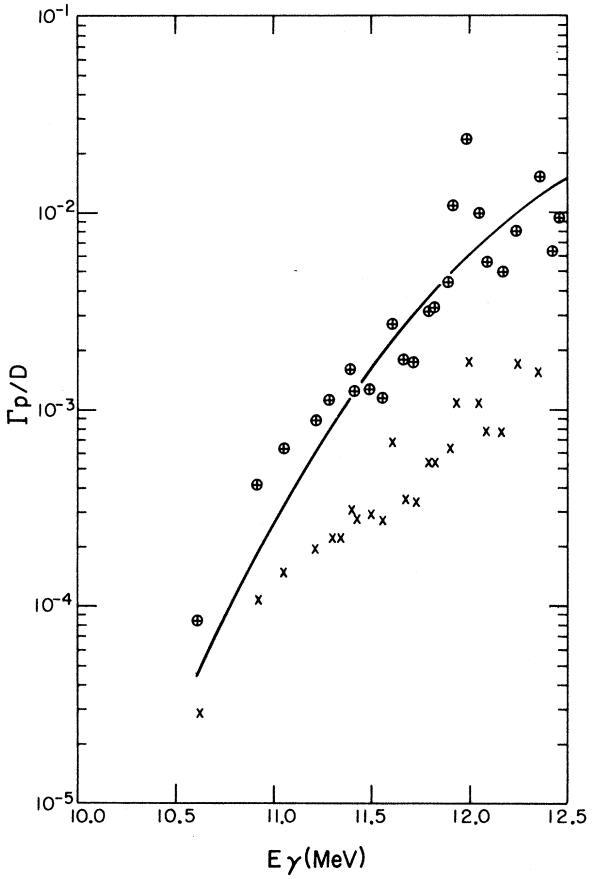

FIG. 5. The photon strength function for ^{89}Y+p. The circled crosses give the value of $\langle\Gamma_p\rangle/D$ if the photon and proton widths of the 1^- states in ^{90}Zr are uncorrelated. The diagonal crosses give the strength function if the widths are completely correlated. The solid line gives the value of $\langle\Gamma_p\rangle/D$ implied for ^{89}Y+p by the Los Alamos average optical-model parameters given in Ref. 33. The proton energy is 8.38 MeV less than the γ-ray energy. The strength function is almost surely dominated by s-wave proton emission, and the s-wave transmission coefficient is therefore approximately given by 2π times the ordinate.

were associated with the excitation of a proton from a $p_{1/2}$ state to an $s_{1/2}$ state.

The dramatic effects which would be expected if there were a common configuration which provided width correlations can be seen near 11.98 MeV in Fig. 5. (It should be emphasized that the argument presented in this paragraph ignores the experimental errors, which are purposely omitted from Fig. 5 to illustrate the information that can be obtained with improved data.) The characteristic signature of a partial width correlation would be a modest increase in photoproton cross section accompanied by a disproportionate drop in elastic scattering such as are found at 11.98 MeV in Table II. The systematic trend at neighboring energies implies an expected ratio of average widths $\langle\Gamma_p\rangle/\langle\Gamma_{\gamma 0}\rangle = 20$, and a cross-section ratio $\sigma_{\gamma p}/\sigma_{\gamma\gamma} = 3$. This systematic trend would imply values of $\sigma_{\gamma\gamma} = 3.6$ mb and $\sigma_{\gamma p} = 10.8$ mb. If 50% of the photon width were correlated with the proton width, this correlated portion would contribute only 0.3 mb while the uncorrelated portion would contribute 1.8 mb to $\sigma_{\gamma\gamma}$. Thus, the result of a 50% correlation would be $\sigma_{\gamma\gamma} = 2.1$ mb (i.e., a 42% decrease) and $\sigma_{\gamma p} = 12.3$ mb (i.e., a 14% increase). The only alternative explanation of a sharp increase of $\sigma_{\gamma p}/\sigma_{\gamma\gamma}$ at 11.98 MeV would be a narrow intermediate structure peak in the proton strength function as shown by the crosses in Fig. 5; if uncorrelated widths are assumed, the proton strength function increases by a factor of 4 in only 100 keV.

The experimental errors associated with the available data preclude the possibility of drawing quantitative conclusions at this time. For example, the 47% statistical error in the elastic-scattering cross section at 11.98 MeV would correspond to a factor of 2 change in the inferred proton strength function. Furthermore, there is an uncertainty in the photoproton cross section caused by a discrepancy in the absolute value of the (p,γ_0) cross section. One group of investigators[21] quotes values which are about 50% higher than the values[20] we used to infer $\sigma_{\gamma t}$ and $\langle\Gamma_p\rangle/D$. (If the photoproton cross sections were increased by 50% at 11.04, 11.49, 11.78, 11.92, and 12.35 MeV the values of $\sigma_{\gamma t}$ would increase by 12, 12, 18, 23, and 25%, respectively, while $\langle\Gamma_p\rangle/D$ would increase by the factors of 2.0, 1.9, 2.0, 2.3, and 2.5, respectively.)

We are planning to remeasure the elastic scattering cross section with higher precision and with a more reliable energy calibration. It would be extremely useful if the ambiguity about the absolute (p,γ_0) cross section and any uncertainties about the relative values[20,21] could also be removed. When these experimental errors are reduced it should be possible to obtain reliable information about $\langle\Gamma_p\rangle/D$ and about correlations. For this purpose, cross sections averaged over about 50 keV would be most useful. Higher-resolution data[20,21] contain additional fluctuations which may well be associated with the limited sample of levels contributing at each energy.

APPENDIX: SOME EFFECTS OF THE PORTER-THOMAS DISTRIBUTION OF WIDTHS ON AVERAGE BRANCHING RATIOS

1. Porter-Thomas Distribution, Enhancement, and Correlations

This Appendix supplements earlier discussions[6-8] of the effects of the Porter-Thomas distribution. It provides previously unavailable numerical results which indicate the size of the effects. In addition, the material below emphasizes the previously unrecognized large enhancement of elastic scattering which occurs when a single dominant competing decay mode also follows a Porter-Thomas distribution. This enhancement makes the average elastic-scattering cross section especially sensitive to width correlations.

A qualitative understanding of the enhancement and a crude estimate of its size can be obtained by examining the Porter-Thomas distribution. This distribution of widths is expected if the amplitude (i.e., the square root of the width) is normally distributed about zero mean. The distribution of a partial width, Γ, about its mean $\langle\Gamma\rangle$ can be expressed conveniently in terms of the dimensionless variable $x^2 \equiv \Gamma/2\langle\Gamma\rangle$,

$$P(x)dx = (2/\pi^{1/2})e^{-x^2}dx . \tag{A1}$$

The enhancement in elastic scattering arises because this distribution includes many very small widths which are balanced by a few large widths. The fraction of levels, f_1, which have widths less than Γ_{f1} can be obtained by integrating Eq. (A1) up to the finite limit corresponding to Γ_{f1}; the definite integral is the error function, erf:

$$f_1 = \mathrm{erf}(\Gamma_{f1}/2\langle\Gamma\rangle)^{1/2} . \tag{A2}$$

The fraction, f_2, of the total cross section that is due to levels whose width exceed Γ_{f2} can be expressed in terms of $z \equiv (\Gamma_{f2}/2\langle\Gamma\rangle)^{1/2}$,

$$f_2 = (2/\pi^{1/2})ze^{-z^2} + (1-\mathrm{erf}\,z) . \tag{A3}$$

A lower limit of the numerical enhancement for any particular case can be obtained easily from Eqs. (A2) and (A3). For example, consider Porter-Thomas distributions of partial ground-state photon widths and of proton widths, where the average values are $\langle\Gamma_{\gamma 0}\rangle = 1$ and $\langle\Gamma_p\rangle = 100$. (If the partial widths did not vary from level to level, or if the proton and photon widths were completely correlated, the ratio of the average cross sections, $\sigma_{\gamma\gamma}/$

$\sigma_{\gamma p}$, would be 1/100.) For a Porter-Thomas distribution, Eq. (A3) can be used to show that 50% of the photon interactions occur in levels with γ-ray widths greater than $2.3\langle\Gamma_{\gamma 0}\rangle$; Eq. (A2) indicates that only 13% of the levels have widths greater than $2.3\langle\Gamma_{\gamma 0}\rangle$. It is easy to see that these levels produce enhanced scattering because their γ-ray widths are above average. Furthermore, when the competing decay mode of proton emission is governed by a Porter-Thomas distribution of widths, there will be many levels with small proton widths. There is more than a 2% chance that the proton width is less than 0.1 (i.e., less than 0.1% of the average value, $\langle\Gamma_p\rangle = 100$). This implies that for 1% of the total interactions (i.e., 2% of 50%) γ emission is more than 23 times more probable than proton emission, implying an enhancement of more than 2300 in elastic scattering (for these few levels). The next 10% of the proton widths have values below 2.3, which implies that γ-ray emission exceeds proton emission for at least another 5% of the interactions. The next 10% of the proton widths have values below 8; when these are compared with the large photon widths responsible for 50% of the absorption, the photon scattering probability exceeds $\frac{1}{5}$. Thus, this crude subdivision of only the smallest 22% of the proton widths and only the 13% largest photon widths clearly indicates that the ratio of photon elastic scattering to photoproton cross section exceeds 4.5/95.5 even though $\langle\Gamma_{\gamma 0}\rangle/\langle\Gamma_p\rangle = 1/100$. The exact analysis given below indicates that a ratio of 21/100 would be expected for $\sigma_{\gamma\gamma}/\sigma_{\gamma p}$ if the widths were uncorrelated. The enhancement of 21 would be reduced dramatically if there were energy regions in which $\Gamma_{\gamma 0}$ and Γ_p are correlated.

2. Quantitative Expressions for Branching Ratios

The average branching ratios can be expressed as a single definite integral,[7] but this integral usually must be evaluated numerically. The following analysis will consider only those cases in which the total width of the ith level is composed of no more than three components,

$$\Gamma_{\gamma t i} = \Gamma_{\gamma 0 i} + \Gamma_{p i} + \Gamma_c , \tag{A4}$$

where $\Gamma_{\gamma 0 i}$ is the partial width for decay to the ground state, $\Gamma_{p i}$ is the partial width for proton decay to a particular residual state, and Γ_c is a constant component which does not vary from one state to another. This constant width, Γ_c, might be the sum of very many small fluctuating widths such as those related to γ-ray decays to many excited states.

The contribution to the elastic scattering from the ith level is proportional to the width ratio $\Gamma_{\gamma 0 i}^2/(\Gamma_{\gamma 0 i} + \Gamma_{p i} + \Gamma_c)$,

$$\sigma_{\gamma\gamma i} \propto \frac{1}{\langle\Gamma_{\gamma 0}\rangle} \frac{\Gamma_{\gamma 0 i}^2}{(\Gamma_{\gamma 0 i} + \Gamma_{p i} + \Gamma_c)} \equiv g . \tag{A5a}$$

The factor $\langle\Gamma_{\gamma 0}\rangle$ is included to make g dimensionless; g would be the ratio of elastic scattering of the ith level to the total photon interaction of a level which had $\Gamma_{\gamma 0} = \langle\Gamma_{\gamma 0}\rangle$. The corresponding expression for the photoproton cross section is used to define a function, h,

$$\sigma_{\gamma p i} \propto \frac{1}{\langle\Gamma_{\gamma 0}\rangle} \frac{\Gamma_{\gamma 0 i}\Gamma_{p i}}{(\Gamma_{\gamma 0 i} + \Gamma_{p i} + \Gamma_c)} \equiv h . \tag{A5b}$$

The cross sections can be averaged over many levels by weighting the expressions in Eq. (A5) with Porter-Thomas distributions for $\Gamma_{\gamma 0}$ and for Γ_p. It is convenient to use dimensionless variables, x^2 and y^2, which are the ratios of the widths to twice the average γ-ray width $\langle\Gamma_{\gamma 0}\rangle$,

$$x_i^2 \equiv \frac{\Gamma_{\gamma 0 i}}{2\langle\Gamma_{\gamma 0}\rangle} , \quad y_i^2 \equiv \frac{\Gamma_{p i}}{2\langle\Gamma_{\gamma 0}\rangle} . \tag{A6}$$

The Porter-Thomas distribution of γ-ray widths is given by Eq. (A1); the average value of $\Gamma_{\gamma 0}/\langle\Gamma_{\gamma 0}\rangle = 2x^2$ is 1.

$$\frac{2}{(\pi)^{1/2}} \int_0^\infty (2x^2) e^{-x^2} dx = 1 . \tag{A7}$$

The corresponding distribution function for y can be expressed in terms of the ratio $\langle\Gamma_p\rangle/\langle\Gamma_{\gamma 0}\rangle \equiv q^2$.

$$P(y)dy = \frac{2}{q(\pi)^{1/2}} e^{-y^2/q^2} dy . \tag{A8}$$

To illustrate how an average value is obtained and simplified, consider the average value of g.

$$\langle g\rangle = \frac{1}{\langle\Gamma_{\gamma 0}\rangle} \int_0^\infty \int_0^\infty \frac{(2x^2\langle\Gamma_{\gamma 0}\rangle)^2}{2x^2\langle\Gamma_{\gamma 0}\rangle + 2y^2\langle\Gamma_{\gamma 0}\rangle + c\langle\Gamma_{\gamma 0}\rangle} \times \frac{4}{\pi q} e^{-x^2} e^{-y^2/q^2} dx dy , \tag{A9}$$

where $c \equiv \Gamma_c/\langle\Gamma_{\gamma 0}\rangle$,

$$\langle g\rangle = \frac{16}{\pi q} \int_0^\infty d\alpha \int_0^\infty dx \int_0^\infty dy\, x^4 e^{-x^2(1+2\alpha)} \times e^{-y^2[(1/q^2)+2\alpha]} e^{-\alpha c} , \tag{A10}$$

$$\langle g\rangle = \int_0^\infty d\alpha \frac{3e^{-\alpha c}}{(1+2\alpha)^{5/2}(1+2q^2\alpha)^{1/2}} . \tag{A11}$$

The average value of h [defined in Eq. (A5b)] can be obtained in the same way,

$$\langle h\rangle = q^2 \int_0^\infty d\alpha \frac{e^{-\alpha c}}{(1+2\alpha)^{3/2}(1+2q^2\alpha)^{3/2}} . \tag{A12}$$

TABLE VII. $\langle \Gamma_p/\Gamma_p+\Gamma_c\rangle = B$, and R as a function of $\Gamma_c/\langle\Gamma_p\rangle$.

$\Gamma_c/\langle\Gamma_p\rangle$ =	0.005	0.01	0.02	0.18	0.405	0.50	0.605
B =	0.916	0.884	0.841	0.609	0.488	0.454	0.424
R =	0.920	0.893	0.858	0.719	0.685	0.681	0.680
$\Gamma_c/\langle\Gamma_p\rangle$ =	0.72	1.28	2	4.50	8	18.18	33.33
B =	0.396	0.307	0.242	0.145	0.0947	0.0478	0.0276
R =	0.681	0.700	0.726	0.797	0.852	0.917	0.948

A direct comparison of Eqs. (A11) and (A12) indicates that in the special case of $q^2 = 1 = \langle\Gamma_p\rangle/\langle\Gamma_{\gamma 0}\rangle$, $\langle g\rangle/\langle h\rangle = \sigma_{\gamma\gamma}/\sigma_{\gamma p} = 3$, independent of Γ_c. However, in general, $\sigma_{\gamma\gamma}$ and $\sigma_{\gamma p}$ must be obtained numerically for each different value of q^2 and c.

The results can be expressed simply for the special case, $\Gamma_c = 0$, because the integrals of Eqs. (A11) and (A12) can be evaluated in closed form. For $\Gamma_c = 0$:

$$\frac{\sigma_{\gamma\gamma}}{\sigma_{\gamma\,\text{total}}} = \langle g\rangle = \frac{2q+1}{(q+1)^2}\,, \tag{A13a}$$

$$\text{enhancement} = \frac{\sigma_{\gamma\gamma}}{\sigma_{\gamma\,\text{total}}}\,\frac{\langle\Gamma_{\gamma 0}\rangle + \langle\Gamma_p\rangle}{\langle\Gamma_{\gamma 0}\rangle} = \left(\frac{2q+1}{q^2+2q+1}\right)(q^2+1), \tag{A13b}$$

$$\frac{\sigma_{\gamma p}}{\sigma_{\gamma\,\text{total}}} = \langle h\rangle = \frac{q^2}{(q+1)^2}\,, \tag{A14a}$$

$$\text{reduction} = \frac{\sigma_{\gamma p}}{\sigma_{\gamma\,\text{total}}}\,\frac{\langle\Gamma_p\rangle + \langle\Gamma_{\gamma 0}\rangle}{\langle\Gamma_p\rangle} = \frac{q^2+1}{q^2+2q+1}\,, \tag{A14b}$$

$$\frac{\sigma_{\gamma\gamma}}{\sigma_{\gamma p}} = \frac{2q+1}{q^2} = \frac{\langle\Gamma_{\gamma 0}\rangle}{\langle\Gamma_p\rangle}\left[1+2\left(\frac{\langle\Gamma_p\rangle}{\langle\Gamma_{\gamma 0}\rangle}\right)^{1/2}\right], \tag{A15a}$$

$$\text{enhancement} = 1+2\left(\frac{\langle\Gamma_p\rangle}{\langle\Gamma_{\gamma 0}\rangle}\right)^{1/2}. \tag{A15b}$$

Equations (A13b) and (A15b) make it clear that the enhancement in elastic scattering due to Porter-Thomas distributions can become arbitrarily large. The possibility of this large enhancement had not been appreciated because earlier work[7] had concentrated on different entrance and exit channels, in which case the reduction factor varies between 0.5 and 1 as indicated in Eq. (A14b).

Other special cases which can be expressed in closed form arise when a single Porter-Thomas distributed width, such as Γ_p or $\Gamma_{\gamma 0}$, competes with a constant width, Γ_c. If the levels are formed by a process unrelated to the width, Γ_p, the average value of the branching ratio, B, can be expressed in terms of $2w^2 = \Gamma_c/\langle\Gamma_p\rangle$.

$$B \equiv \left\langle \frac{\Gamma_p}{\Gamma_p+\Gamma_c}\right\rangle = 1-(\pi)^{1/2}\, w\, e^{w^2}(1-\operatorname{erf} w). \tag{A16}$$

TABLE VIII. The enhancement in the ratio $\sigma_{\gamma\gamma}/\sigma_{\gamma p}$ due to uncorrelated Porter-Thomas distributions. The values given are $(\sigma_{\gamma\gamma}/\sigma_{\gamma p})/(\langle\Gamma_{\gamma 0}\rangle/\langle\Gamma_p\rangle)$.

$\Gamma_c/\langle\Gamma_{\gamma 0}\rangle = c$ / $q^2 = \langle\Gamma_p\rangle/\Gamma_{\gamma 0}$	32	16	8	4	2	1	1/2	1/4	0
128	8.72	10.94	13.48	16.06	18.41	20.28	21.59		23.63
64	6.72	8.24	9.98	11.77	13.38	14.68	15.59	16.19	17.00
32	5.34	6.36	7.54	8.74	9.84	10.72	11.34	11.75	12.31
16	4.40	5.06	5.81	6.62	7.35	7.93	8.35	8.62	9.00
8	3.77	4.17	4.65	5.15	5.60	5.97	6.23	6.41	6.66
4	3.38	3.59	3.85	4.13	4.39	4.60	4.75	4.85	5.00
2	3.14	3.22	3.33	3.45	3.56	3.65	3.71	3.76	3.83
1	3.00	3.00	3.00	3.00	3.00	3.00	3.00	3.00	3.00
1/2	2.93	2.87	2.80	2.72	2.64	2.57	2.51	2.47	2.41
1/4	2.89	2.80	2.69	2.56	2.42	2.29	2.19	2.12	2.00
1/8		2.77	2.63	2.46	2.29	2.12	1.98	1.88	1.71
1/16			2.60	2.41	2.21	2.02	1.86	1.73	1.50
1/32				2.39	2.17	1.97	1.79	1.64	1.35
1/64					2.15	1.94	1.75	1.59	1.25
1/128						1.92	1.73	1.56	1.18

TABLE IX. The ratios R_1, R_2, and R_3 for uncorrelated Porter-Thomas distributions.

q^2		$c=32$	$c=16$	$c=8$	$c=4$	$c=2$	$c=1$	$c=1/2$	$c=1/4$
128	R_1	0.0012	0.0034	0.0093	0.024	0.057	0.129	0.278	
	R_2	0.0171	0.040	0.088	0.190	0.397	0.816	1.65	
	R_3	0.586	0.692	0.782	0.854	0.908	0.945	0.969	
64	R_1	0.0014	0.0043	0.012	0.031	0.076	0.173	0.375	0.788
	R_2	0.0137	0.0336	0.077	0.170	0.363	0.753	1.54	3.11
	R_3	0.487	0.604	0.715	0.806	0.876	0.925	0.957	0.977
32	R_1	0.0017	0.0053	0.015	0.040	0.197	0.226	0.496	1.04
	R_2	0.0103	0.027	0.065	0.147	0.320	0.675	1.39	2.83
	R_3	0.386	0.514	0.638	0.749	0.837	0.901	0.943	0.969
16	R_1	0.0020	0.0063	0.018	0.050	0.125	0.289	0.635	1.34
	R_2	0.0072	0.020	0.051	0.121	0.271	0.583	1.22	2.49
	R_3	0.294	0.420	0.556	0.684	0.781	0.871	0.925	0.958
8	R_1	0.0022	0.0072	0.022	0.060	0.152	0.358	0.792	1.69
	R_2	0.0046	0.0138	0.037	0.094	0.218	0.479	1.017	2.10
	R_3	0.218	0.336	0.474	0.615	0.740	0.837	0.904	0.946
4	R_1	0.0023	0.0079	0.025	0.070	0.180	0.428	0.956	2.05
	R_2	0.0028	0.0088	0.026	0.067	0.164	0.372	0.805	1.68
	R_3	0.163	0.267	0.401	0.548	0.687	0.800	0.881	0.933
2	R_1	0.0024	0.0084	0.027	0.078	0.204	0.493	1.114	2.40
	R_2	0.0015	0.0052	0.016	0.045	0.115	0.270	0.600	1.27
	R_3	0.127	0.218	0.343	0.491	0.638	0.764	0.857	0.918
1	R_1	0.0025	0.0087	0.028	0.083	0.224	0.548	1.25	2.71
	R_2	0.00083	0.0029	0.0094	0.028	0.075	0.183	0.417	0.91
	R_3	0.106	0.186	0.302	0.446	0.597	0.731	0.834	0.904
1/2	R_1	0.0025	0.0089	0.029	0.087	0.238	0.590	1.36	1.60
	R_2	0.00043	0.00155	0.0052	0.0161	0.0450	0.115	0.270	0.595
	R_3	0.094	0.167	0.275	0.414	0.565	0.704	0.814	0.891
1/4	R_1	0.0025	0.0090	0.030	0.090	0.247	0.617	1.43	3.14
	R_2	0.00022	0.00080	0.0028	0.0088	0.0255	0.0674	0.167	0.371
	R_3	0.088	0.157	0.260	0.395	0.544	0.685	0.799	0.881
1/8	R_1		0.0091	0.030	0.091	0.252	0.635	1.48	3.27
	R_2		0.00041	0.0014	0.0046	0.0138	0.0374	0.0934	0.217
	R_3		0.152	0.252	0.384	0.531	0.672	0.789	0.873
1/16	R_1			0.030	0.092	0.255	0.645	1.51	3.35
	R_2			0.0073	0.0024	0.0072	0.0199	0.0508	0.120
	R_3			0.247	0.378	0.524	0.665	0.782	0.867
1/32	R_1				0.092	0.256	0.650	1.53	3.38
	R_2				0.00121	0.0037	0.0103	0.0267	0.065
	R_3				0.375	0.520	0.661	0.778	0.864
1/64	R_1					0.257	0.653	1.54	3.41
	R_2					0.00186	0.0053	0.0137	0.035
	R_3					0.518	0.658	0.776	0.862
1/128	R_1						0.654	1.54	3.43
	R_2						0.0027	0.0070	0.017
	R_3						0.657	0.774	0.861

Because most levels would have values of Γ_p lower than $\langle\Gamma_p\rangle$ (due to the assumed-Porter-Thomas distribution), the probability of proton-emission, B, would be lower than that implied by the ratio of the average widths by a reduction factor, R.

$$R \equiv \left\langle \frac{\Gamma_p}{\Gamma_p+\Gamma_c} \right\rangle \Big/ \frac{\langle\Gamma_p\rangle}{\langle\Gamma_p\rangle+\Gamma_c} = (1+2w^2)B. \qquad \text{(A17)}$$

Numerical values of B and R are given in Table VII. If the channel corresponding to the Porter-Thom-

as width distribution is the entrance channel, elastic scattering is enhanced by a factor, E_1. This enhancement can be expressed analytically by exploiting the identity, $\langle \Gamma_p^2/(\Gamma_p+\Gamma_c)\rangle = \langle \Gamma_p\rangle - \Gamma_c B$. In order to interpret elastic photon scattering, it will be helpful to redefine $2w^2 = \Gamma_c/\langle \Gamma_{\gamma 0}\rangle$; the enhancement, E_1, can then be expressed as

$$E_1 = \left\langle \frac{\Gamma_{\gamma 0}{}^2}{\Gamma_{\gamma 0}+\Gamma_c} \right\rangle \Big/ \frac{\langle \Gamma_{\gamma 0}\rangle^2}{\langle \Gamma_{\gamma 0}\rangle + \Gamma_c} = 1 + 2w^2(1-R). \tag{A18}$$

The enhancement factor, E_1, is given in Table IV in Sec. IV A of the main text; it varies between the value of 3, which is attained when $\Gamma_c/\langle \Gamma_{\gamma 0}\rangle$ is very large and the value of 1 which is the value of E_1 when $\Gamma_c/\langle \Gamma_{\gamma 0}\rangle$ approaches zero.

In the general case when the three widths, $\Gamma_{\gamma 0}$, Γ_p, and Γ_c, are finite, the cross sections can be obtained by evaluating the integrals of Eqs. (A11) and (A12) numerically. The ratio of elastic scattering, $\sigma_{\gamma\gamma}$, to photoproduction, $\sigma_{\gamma p}$, is enhanced over the ratio $\langle \Gamma_{\gamma 0}\rangle/\langle \Gamma_p\rangle$ by a factor which varies with $q^2 = \langle \Gamma_p\rangle/\langle \Gamma_{\gamma 0}\rangle$ and with $c = \Gamma_c/\langle \Gamma_{\gamma 0}\rangle$. These enhancement factors are listed in Table VIII for 15 values of q^2 and for 9 values of c. For $q^2 > 1$, the enhancements become larger as Γ_c decreases; for $q^2 < 1$, the enhancements decrease as Γ_c decreases. The enhancements shown in Table VIII due to two uncorrelated Porter-Thomas distributions illustrate the sensitivity of elastic scattering to correlations because the enhancements would be reduced if the proton widths were correlated with the photon widths. If one enters an energy region where these widths are correlated, the photoproton cross section would grow and the elastic scattering cross section would decrease. The elastic scattering cross section would be particularly sensitive if the enhancement factors are large because the elastic scattering might then be decreased by the entire enhancement factor even though the photoproton cross section might increase by only a modest percentage.

The results of the numerical calculations can be presented in a form that is convenient for the interpretation of measured elastic scattering and photoproton cross sections. Equations (10) and (14) of the text indicate that the experimental cross sections can be converted (with the aid of an assumed value of D/Γ_c) to the width ratios:

$$R_1 = \frac{1}{\Gamma_c}\left\langle \frac{\Gamma_{\gamma 0}{}^2}{\Gamma_{\gamma 0}+\Gamma_p+\Gamma_c} \right\rangle, \tag{A19}$$

$$R_2 = \frac{1}{\Gamma_c}\left\langle \frac{\Gamma_{\gamma 0}\Gamma_p}{\Gamma_{\gamma 0}+\Gamma_p+\Gamma_c} \right\rangle. \tag{A20}$$

These width ratios can be used to determine $\Gamma_c/\langle \Gamma_{\gamma 0}\rangle$ and $\langle \Gamma_p\rangle/\langle \Gamma_{\gamma 0}\rangle$. In addition, these values can be used to find the ratio of the observed cross section to the total γ-ray interaction cross section,

$$R_3 = \frac{\sigma_{\gamma\gamma}+\sigma_{\gamma p}}{\sigma_{\gamma t}}. \tag{A21}$$

Table IX presents an array of R_1, R_2, and R_3 for discrete values of c and q^2. The numerical values given in the text for $\sigma_{\gamma t}$ were obtained by plotting both R_2 and R_3 as a function of R_1 on log-log paper with c and q^2 as parameters. The measured values of R_1 and R_2 determine R_3 relatively precisely; R_3 is determined relatively well by the ratio of R_1 to R_2 so that errors in the assumed value D/Γ_c are not too important.

---

†Work supported by the Office of Naval Research and The National Science Foundation Grant No. NSF GP 9312. The experimental data were originally presented in a thesis which fulfilled, in part, the requirements for a Ph.D.

*Present address: Rensselaer Polytechnical Institute, Troy, New York.

[1]E. G. Fuller and E. Hayward, Phys. Rev. 101, 692 (1956).

[2]K. Reibel and A. K. Mann, Phys. Rev. 118, 701 (1960).

[3]T. Tohei, M. Sugawara, S. Mori, and M. Kumara, J. Phys. Soc. Japan 16, 1657 (1961). (Note that Ref. 4 includes suggested corrections to the results of this paper.)

[4]M. Sugawara, S. Mori, A. Ono, A. Hotta, and M. Kimura, J. Phys. Soc. Japan 18, 17 (1963).

[5]H A. Bethe and J. Ashkin, *Experimental Nuclear Physics*, edited by E. Segrè (John Wiley & Sons, Inc., New York, 1953), Vol. 1, p. 346.

[6]A. M. Lane and J. E. Lynn, Proc. Phys. Soc. (London) A70, 557 (1957).

[7]P. A. Moldauer, Phys. Rev. 123, 968 (1961).

[8]P. Axel, Phys. Rev. 126, 671 (1962).

[9]L. M. Bollinger, in *Proceedings of the International Symposium on Nuclear Structure, Dubna, 1968* (International Atomic Energy Agency, Vienna, Austria, 1969), p. 317.

[10]J. S. O' Connell, P. A. Tipler, and P. Axel, Phys. Rev. 126, 228 (1962).

[11]P. A. Tipler, P. Axel, N. Stein, and D. C. Sutton, Phys. Rev. 129, 2096 (1963).

[12]P. Axel, Phys. Letters 4, 320 (1963).

[13]B. L. Berman, J. T. Caldwell, R. R Harvey, M. A. Kelly, R. L. Bramblett, and S. C. Fultz, Phys. Rev. 162, 1098 (1967).

[14]P. Axel, K. Min, N. Stein, and D. C. Sutton, Phys. Rev. Letters 10, 299 (1963).

[15]K. Izumo, Progr. Theoret. Phys. (Kyoto) 26, 807 (1961); S. Izarasi, K. Izumo, and T. Udagawa, Progr. Theoret. Phys. (Kyoto) 21, 468 (1959).

[16]B. Block and H. Feshbach, Ann. Phys. (N.Y.) 23, 47 (1963); A. Kerman, L. S. Rodberg, and J. E. Young, Phys. Rev. Letters 11, 422 (1963); C. Shakin, Ann. Phys. (N.Y.) 22, 373 (1963); R. H. Lemmer, Phys. Letters 4, 205 (1963).

[17]H. Feshbach, A. K. Kerman, and R. H. Lemmer, Ann. Phys. (N.Y.) 41, 230 (1967).
[18]P. Axel, in *Proceedings of the International Symposium on Nuclear Structure, Dubna, 1968* (International Atomic Energy Agency, Vienna, Austria, 1969), p. 299.
[19]E. Obst, F. Rauch, and E. Rossle, Phys. Letters 21, 50 (1966).
[20]E Obst, F. Rauch, and H. G. Wahsweiler, Nucl. Phys. A103, 17 (1967).
[21]W. M. Mason, G. Kernel, J. L. Black, and N. W. Tanner, Nucl. Phys. A135, 193 (1969).
[22]M. Beer, M. A. Lone, R. E. Chrien, O. A. Wasson, M. R. Bhat, and H. R. Muether, Phys. Rev. Letters 20, 340 (1968); in *Proceedings of the International Symposium on Nuclear Structure, Dubna, 1968* (International Atomic Energy Agency, Vienna, Austria, 1969), pp. 342–343.
[23]J. S. O' Connell, Rev. Sci. Instr. 32, 1314 (1961).
[24]T. Fuketa, F. A. Khan, and J. A. Harvey, Bull. Am. Phys. Soc. 8, 71 (1963).
[25]A. Gilbert and A. G. W. Cameron, Can. J. Phys. 43, 1446 (1965).
[26]D. B. Thomson, Phys. Rev. 129, 1649 (1963).
[27]S. C. Fultz, B. L. Berman, J. T. Caldwell, R. L. Bramblett, and M. A. Kelly, Phys. Rev. 186, 1270 (1969).
[28]L. M. Bollinger, in *Nuclear Spectroscopy*, edited by F. Ajzenberg-Selove (Academic Press Inc., New York, 1960), Part A, p. 444.
[29]H. Shwe and R. E. Cote, Phys. Rev. 179, 1148 (1969).
[30]J. Kim, J. A. Biggerstaff, and W. M. Good, Bull. Am. Phys. Soc. 8, 556 (1963); S. S. Moskalev, H. V. Muradien, and Y. V. Adamchuk, Nucl. Phys. 53, 667 (1964).
[31]G. Vourvopoules and J. D. Fox, Phys. Rev. 177, 1558 (1969).
[32]H. E. Jackson, Phys. Rev. 131, 2153 (1963).
[33]The quoted transmission coefficients were calculated using the optical-model parameters given in L. Rosen, J. G. Beary, A. S. Goldhaber, and E. H. Auerbach, Ann. Phys. (N.Y.) 34, 96 (1965).
[34]C. H. Johnson and R. L. Kernell, Phys. Rev. Letters 23, 20 (1969).

PHYSICAL REVIEW C VOLUME 2, NUMBER 2 AUGUST 1970

Effect of Nuclear Deformability on Reaction Cross Sections*

Peter W. Riesenfeldt and T. Darrah Thomas

Department of Chemistry, Princeton University, Princeton, New Jersey 08540
and Princeton-Pennsylvania Accelerator, Princeton, New Jersey 08540
(Received 12 March 1970)

We have calculated the effect of nuclear deformability on the cross section for interaction of heavy ions with uranium. Static calculations indicate that these effects should be large; dynamic calculations with liquid-drop parameters indicate that they should be smaller, but measurable with currently available heavy ions (argon incident on uranium). Dynamic calculations with parameters derived from spectroscopic measurements indicate that the effects should be quite small, in agreement with experiment. We have done both classical and quantum-mechanical calculations; the two methods give the same results. The quantum-mechanical calculations also give the probability of Coulomb excitation to the vibrational states of the target nucleus. We discuss the value of several approximations used to estimate total reaction cross sections.

I. INTRODUCTION

Proposed experiments to synthesize the superheavy elements ($Z \approx 114$) will combine very heavy ions as projectiles with heavy element targets. For such experiments to be successful, it is necessary that the projectile and target fuse to form a compound nucleus and that the nucleus so formed dissipate its excitation energy in neutron or γ-ray emission rather than in fission.

The probability for fission is enhanced if several neutrons are emitted, since competition between neutron emission and fission occurs at each stage of evaporation. This probability is also enhanced by the high angular momenta characteristic of heavy-ion-induced reactions. In order to maximize the chance that the nucleus of interest survives fission, it is desirable that the initial compound nucleus have as low an energy and angular momentum as possible. These requirements dictate that the kinetic energy of the incident projectile be as low as possible.

A low energy for the projectile is desirable from another point of view. It is believed that the probability for incomplete fusion reactions increases with increasing kinetic energy. Experimental support for this idea is found in the work of Jodogne, Kowalski, and Miller[1] who investigated the probability for complete fusion as a function of energy for several light element systems. They found not only that the fraction of reactions leading to complete fusion decreases with increasing energy